Downscaled CMIP3 and CMIP5 Climate Projections - Addendum

Release of Downscaled CMIP5 Climate Projections (LOCA) and Comparison with Preceding Information

Bureau of Reclamation

California Energy Commission

Climate Analytics Group

Climate Central

Lawrence Livermore National Laboratory

NASA's Ames Research Center, Moffett Field, CA

Santa Clara University

Scripps Institution of Oceanography

U.S. Army Corps of Engineers

U.S. Geological Survey

Cooperative Institute for Research in Environmental Sciences

Downscaled CMIP3 and CMIP5 Climate Projections - Addendum

Release of Downscaled CMIP5 Climate Projections (LOCA) and Comparison with Preceding Information

September 2016

Authored by:

Cameron Bracken, Bureau of Reclamation

Review and Contributions from:

Jeff Arnold, U.S. Army Corps of Engineers
Dan Cayan, Scripps Institution of Oceanography, University of California San Diego and U.S. Geological Survey
Subhrendu Gangopadhyay, Bureau of Reclamation
Ethan Gutmann, National Center for Atmospheric Research
Ben Livneh, Cooperative Institute for Research in Environmental Sciences, University of Colorado
Ed Maurer, Santa Clara University
Kenneth Nowak, Bureau of Reclamation
David Pierce, Scripps Institution of Oceanography, University of California San Diego
Tom Pruitt, Bureau of Reclamation
Andy Wood, National Center for Atmospheric Research

Prepared for:

Users of the "Downscaled CMIP3 and CMIP5 Climate and Hydrology Projections: Release of Downscaled CMIP5 Climate Projections" website at: http://gdo-dcp.ucllnl.org/downscaled_cmip_projections/.

Table of Contents

Page

Tables

Page

Figures

Page

1 Acknowledgements

1.1 Support provided by

Development and production of LOCA and attendant bias correction components has been sponsored by the California Energy Commission, the U.S. Army Corps of Engineers, the U.S. Geological Survey via the Climate Science Centers and the GEODATA Portal Center for Integrated Data Analytics, NOAA via the California Nevada Applications Program RISA, and the Bureau of Reclamation Research and Development Office. Historical gridded temperature and precipitation data were provided by Dr. Ben Livneh, University of Colorado. Major parts of LOCA were produced on the NASA Earth Exchange (NEX), who provided key computational resources and support. Additional computational resources were provided by Dr. John Helly of the San Diego Supercomputer Center.

1.2 Acknowledgements and Citation of these Projections

When publishing research based on projections from this archive, please include two acknowledgements:

1. Acknowledge the superseding effort:

    a. For Coupled Model Intercomparison Project phase 3 (CMIP3), the following is language suggested by the CMIP3 archive hosts at the Program for Climate Model Diagnosis and Intercomparison (PCMDI):

    "We acknowledge the modeling groups, the Program for Climate Model Diagnosis and Intercomparison (PCMDI), and the World Climate Research Programme (WCRP) Working Group on Coupled Modelling (WGCM) for their roles in making available the WCRP CMIP3 multi-model dataset. Support of this dataset is provided by the Office of Science, U.S. Department of Energy."

    PCMDI also requests that in first making reference to the projections from this archive, please first reference the CMIP3 dataset by including the phrase "the World Climate Research Programme's (WCRP's) Coupled Model Intercomparison Project phase 3 (CMIP3) multi-model dataset." Subsequent references within the same publication might refer to the CMIP3 data with terms such as "CMIP3 data," "the CMIP3 multi-model dataset," "the CMIP3 archive," or the "CMIP3 dataset."

    b. For Coupled Model Intercomparison Project phase 5 (CMIP5), the model output should be referred to as "the CMIP5 multi-model ensemble [archive/output/results/of simulations/dataset/ ...]." In publications, you should include a table (referred to below as Table XX) listing the models and institutions that provided model output used in your study. In this table, and as appropriate in figure legends, you should use the CMIP5 "official" model names found in "CMIP5 Modeling Groups and their Terms of Use" (http://cmip-pcmdi.llnl.gov/cmip5/docs/CMIP5_modeling_groups.pdf). In addition, an acknowledgment similar to the following should be included in your publication:

"We acknowledge the World Climate Research Programme's Working Group on Coupled Modelling, which is responsible for CMIP, and we thank the climate modeling groups (listed in Table XX of this paper) for producing and making available their model output. For CMIP, the U.S. Department of Energy's Program for Climate Model Diagnosis and Intercomparison provides coordinating support and led development of software infrastructure in partnership with the Global Organization for Earth System Science Portals."
where "Table XX" of your paper should list the models and modeling groups that provided the data you used. In addition, it may be appropriate to cite one or more of the CMIP5 experiment design articles listed on the CMIP5 reference page.

2. Second, generally acknowledge this archive as "Downscaled CMIP3 and CMIP5 Climate and Hydrology Projections" archive at: http://gdo-dcp.ucllnl.org/downscaled_cmip_projections. To reference specific statistically downscaled climate and hydrology data from the archive, please use the following references:

    a. *for BCSD CMIP3 climate*: Maurer, E.P., L. Brekke, T. Pruitt, and P.B. Duffy, 2007, "Fine-resolution climate projections enhance regional climate change impact studies," Eos Trans. AGU, 88(47), 504.

    b. *for BCSD CMIP3 hydrology*: Reclamation, 2011, West-Wide Climate Risk Assessments: Bias-Corrected and Spatially Downscaled Surface Water Projections, Technical Memorandum No. 86-68210-2011-01, prepared by the U.S. Department of the Interior, Bureau of Reclamation, Technical Services Center, Denver, Colorado, 138 p.

    c. *for BCSD CMIP5 climate*: Provide citation to: Reclamation, 2013. Downscaled CMIP3 and CMIP5 Climate Projections: Release of Downscaled CMIP5 Climate Projections, Comparison with Preceding Information, and Summary of User Needs. U.S. Department of the Interior, Bureau of Reclamation, 104 p., available at: http://gdo-dcp.ucllnl.org/downscaled_cmip_projections/techmemo/downscaled_climate.pdf.

    d. *for BCSD CMIP5 hydrology*: Reclamation, 2014. Downscaled CMIP3 and CMIP5 Hydrology Projections - Release of Hydrology Projections, Comparison with Preceding Information, and Summary of User Needs. U.S. Department of the Interior, Bureau of Reclamation,104 p., available at: http://gdo-dcp.ucllnl.org/downscaled_cmip_projections/techmemo/downscaled_climate.pdf.

    e. *for the locally constructed analogs method (LOCA) CMIP5 projections*: Pierce, D. W., D. R. Cayan, and B. L. Thrasher, Statistical Downscaling Using Localized Constructed Analogs (LOCA)*, Journal of Hydrometeorology, 15(6), 2558-2585, 2014; and Pierce, D. W., D. R. Cayan, E. P. Maurer, J. T. Abatzoglou, and K. C. Hegewisch, 2015: Improved bias correction techniques for hydrological simulations of climate change. J. Hydrometeorology, v. 16, p. 2421-2442. DOI: http://dx.doi.org/10.1175/JHM-D-14-0236.1

2 This Addendum

This document is an addendum to the report "Downscaled CMIP3 and CMIP5 Climate Projections: Release of Downscaled CMIP5 Climate Projections, Comparison with Preceding Information, and Summary of User Needs" [*Bureau of Reclamation,* 2013]. The reader is referred to that document for full descriptions of the CMIP archives as well as the BCCA and BCSD methods. For further details the reader is referred to the original citations for each downscaling method, listed below in the Introduction section. This report provides a high level introduction to three down-scaling methods and a comparison of the methods for selected meteorological variables.

3 LOCA Addition to Archive

Table 1 shows CMIP5 models downscaled with the LOCA method and provided in the archive; 32 models are included, with both RCP 4.5 and RCP 8.5 runs. CMIP uses a series of letters and numbers to distinguish different model runs composing an ensemble. A single ensemble member is included from each model, generally, member "r1i1p1". However, some models only had the requisite daily data available from a different ensemble member, in which case that ensemble member was used instead. For example, models CCSM4, GISS-E2-R, and GISS-E2-H used ensemble member "r6i1p1" over the historical period, the ensemble member used appears in the name of the LOCA data file.

Table 1: CMIP5 models provided in the archive for run r1i1p1 only.

Model	Model	Model
access1-0	csiro-mk3-6-0	inmcm4
access1-3	ec-earth	ipsl-cm5a-lr
bcc-csm1-1	fgoals-g2	ipsl-cm5a-mr
bcc-csm1-1-m	gfdl-cm3	miroc-esm
canesm2	gfdl-esm2g	miroc-esm-chem
ccsm4	gfdl-esm2m	miroc5
cesm1-bgc	giss-e2-h	mpi-esm-lr
cesm1-cam5	giss-e2-r	mpi-esm-mr
cmcc-cm	hadgem2-ao	mri-cgcm3
cmcc-cms	hadgem2-cc r	noresm1-m
cnrm-cm5	hadgem2-es	

4 Introduction

The purpose of this report is to provide a high level introduction and comparison of three daily datasets of downscaled climate projections from the Coupled Model Intercomparison Project phase 5 (CMIP5). The three datasets are based on the following downscaling methods:

- Localized Constructed Analogs (LOCA) [*Pierce et al.,* 2014]
- Bias correction with spatial disaggregation (BCSDm) [*Wood et al.,* 2004]
- Bias correction with constructed analogs (BCCA) [*Maurer et al.,* 2010]

This document accompanies the public release of the dataset produced with the localized constructed analogs (LOCA) method [*Pierce et al.*, 2014] and is intended as a companion to the 2013 Bureau of Reclamation report titled "Downscaled CMIP3 and CMIP5 Climate Projections" [*Bureau of Reclamation*, 2013]. The methods comparison includes three daily variables: precipitation *(P)*; maximum temperature $(T_{max})_t$; and minimum temperature (T_{min}). This document is intended to present several salient features of these datasets but not to be an exhaustive comparison between the downscaled datasets presented here.

4.1 Clarification of Terminology

Bureau of Reclamation [2013] referred to various downscaling methods with the use of number "5" appended to the method name, denoting the downscaling of CMIP5 projections (as opposed to CMIP3). In this report, all the methods evaluated use CMIP5 projections; so the use of the appended number "5" is omitted. Additionally, the bias correction with spatial disaggregation method is referred as BCSDm (following *Gutmann et al.* [2014]) to distinguish it from a variation of BCSD that is applied directly at a daily time step (BCSDd) [*Thrasher et al.*, 2012].

5 Spatial Downscaling and Bias Correction Methods

5.1 Spatial Downscaling

Spatial downscaling refers to techniques that impart a finer resolution spatial structure to coarse resolution output of global climate models (GCMs). There are two predominant types of spatial downscaling – dynamical and statistical. Dynamical methods use GCM output as boundary conditions for finer resolution regional climate models, linking process-based physical relationships between small and large scale behavior. While these methods may capture (possibly unobserved) nonstationary behaviors, they are computationally expensive and are not practical for downscaling of the large ensembles of century-long GCM runs that are of interest in many modern studies, on the continental scale. Statistical downscaling methods rely on historically observed statistical relationships between coarse- and fine-spatial scale patterns. Statistical methods typically produce a smaller set of output variables than dynamical methods but are much less computationally expensive. The three methods evaluated in this report are statistical techniques.

5.2 Bias Correction

Bias correction (BC) refers to techniques for removing the systematic errors ("biases") that all GCMs produce in their output fields. Depending on the method, bias correction can be a separate step that is independent from the spatial downscaling (which is true for the methods described here) or an implicit part of the spatial downscaling technique. In the latter event the entire process is often simply termed "downscaling". Here the steps are separate, so the term "downscaling" refers specifically to the spatial downscaling process, and the bias correction used in LOCA is described separately in section 5.3.2.

5.3 Localized Constructed Analog (LOCA)

Constructed Analog (CA) methods spatially downscale a GCM day by searching for a set of observed days that are similar to the GCM day when the observations are coarsened to the GCM grid (e.g., Hidalgo et al., 2008). The matching observed days are called *analog days* because they are analogous to the model day being spatially downscaled. Often, about 30 analog days are identified for each model day being downscaled. The original fine-resolution observations from the selected analog days are then combined to form the final spatially downscaled field; exactly how this is done depends on the method.

In previous constructed analog techniques such as BCCA (e.g., Hidalgo et al., 2008) and MACA (Abatzoglou and Brown, 2012), the analog days represent the best matches (least RMSE) between the model and observed day evaluated over the entire domain being downscaled. The analog days are then combined by computing optimal weights such that the weighed sum of the analog days best reproduces the model day being downscaled. These same weights are then applied to the original fine-resolution observations from the analog days, producing the final spatially downscaled field (Maurer et al., 2010). A drawback of this approach is that as the domain size increases (say, to the size of the contiguous U.S. [CONUS]), it becomes increasingly difficult to find good analog days for the entire domain. Also, when downscaling precipitation, it becomes more likely that some of the analog days will have precipitation where the model day has none, which tends to produce spurious drizzle. Finally, linearly combining multiple analog days based on the best match over a large domain tends to miss localized extreme precipitation events, which can be critical to impacts.

To address these issues a localized version of constructed analogs, LOCA, was developed (Pierce et al., 2014). Details are given below, but the key differences changes in LOCA are: 1) LOCA selects the 30 analog days in a synoptic-scale (~1000 km) region around the point being spatially downscaled to rather than across the entire domain. Different points in the domain will then be using different analog days. So, for example, there is no requirement that the observed analog day simultaneously match the model's precipitation in Seattle and Miami, locations far enough away from each other that there is no meaningful physical connection between their weather. 2) Once the 30 analog days are selected, the *one* analog day of the 30 that best matches the model in a small area (~100 km) around the point being downscaled is chosen as the final analog day to use in that small area. Using only one analog day instead of a weighted sum of many analog days avoids the problems with spurious drizzle generation and damping of localized precipitation extremes. A key point of LOCA is that the final chosen analog day is the closest match to the GCM day over both synoptic length scales (~1000 km) and in the immediate neighborhood of the point being downscaled (~100 km).

5.3.1 LOCA Spatial Downscaling Procedure

Step 1. Develop analog pool points and spatial masks

As noted above, LOCA differs from previous constructed analog techniques in its selection of analog days in a region (~1000 km) around the point being downscaled instead of over the entire domain. Conceptually, this could be done at every point. However selecting the analog days is the most computationally expensive part of constructed analog techniques. Going from selecting 30 analog days for the *entire domain* (as done in BCCA) to 30 analog days *at each point* would be computationally prohibitive. It is also unnecessary, since the weather conditions in a 1000-km length scale region centered on, say, Los Angeles are almost identical to the weather conditions in a similar region centered on San Diego. Very nearly the same 30 analog days would be picked for both locations.

For computational efficiency, the 30 analog days are picked at a subset of points called the "analog pool points." The analog pool points for a domain in the western U.S. are indicated by Xs in Figure 1. The same analog days are then used at all nearby coarse grid cells, as indicated by the colors in Fig. 1. *Pierce et al.* [2014] conclude that the exact placement of the analog pool points does not matter as long as they are not too far apart (about 1 analog pool point per 3°x3° region), and the distribution is approximately equal across the domain. Again, developing the analog pool location is only done once for a given coarse grid.

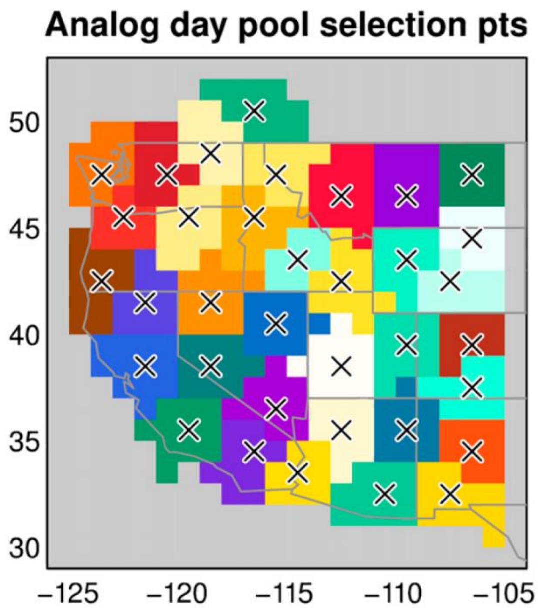

Figure 1. Crosses indicate the analog day pool selection points; colors indicate the domain over which a point is used. *Source: Pierce et al.* [2014]. Note although this figure shows only the western United States, LOCA projections are available for the contiguous United States (CONUS).

Step 2. Select analog days at the regional scale

Up to now, it has been left vague exactly what surrounding ~1000 km length scale region LOCA uses when selecting the 30 analog days. (Again, for computational efficiency, this selection is done only at the analog day pool selection points.) One could, for example, use a simple circle with radius 1000 km centered on the analog pool point, and evaluate over that circle the RMSE match between each observed day and model day being downscaled. However, the idea of LOCA is that the selected analog days should be relevant to the point being downscaled. For example, if downscaling to Seattle, it is not relevant what the weather is in Miami, so the region used to pick the analog day should exclude Miami. On the other hand, the weather in Portland OR is likely related to the weather in Seattle, so Portland should be included in the region used to select analog days for Seattle.

This motivates choosing the region for analog day selection to be locations where the weather is related to the point being downscaled. In the version of LOCA used to generate the data in the archive, a very simple criterion was used: a location is included if the Pearson correlation between the time series of the variable at that location and the time series of the variable at the point being downscaled is positive (anomalies are used in this calculation for temperature). This correlation is evaluated individually for every variable and every season [December-February (DJF), March-May (MAM), June-August (JJA), and September-November (SON)].

As an example, the pink area in Figure 2 shows the domain used for picking analog days for a location near Seattle (cross) when downscaling precipitation in MAM. Contours in Figure 2 show the correlation values > 0 between time series of MAM precipitation at Seattle and all other locations in the western U.S. Using a cutoff of zero is conservative in the sense that a relatively wide region is considered when forming the analogs, which makes LOCA's analog day selection process a less drastic change from the existing BCCA approach. Other approaches, such as using smaller regions based on correlation values that pass a statistical significance test, could also be contemplated. (Although it should be noted that given a training data set consisting of 50 years of daily data, significant correlations are in the range of 0.05, even taking typical synoptic timescales into account.)

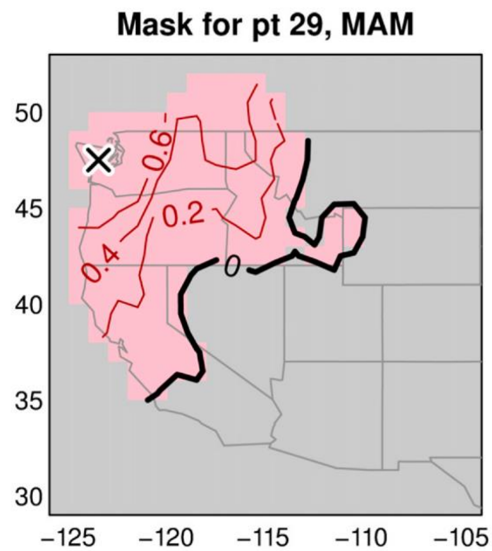

Figure 2. Example spatial mask for spring (MAM) precipitation at analog pool point 29 (cross). Pink area shows where the mask is 1; gray areas show where the mask is 0. The mask is set to 1 at every location that has a Pearson correlation with the time series at the analog pool point that is > 0. Contour lines show correlation coefficient values between the time series at the analog point location (cross) and all other points in the domain. *Source: Pierce et al.* [2014].

The match between the model day being downscaled and the observed day is measured using the root-mean-square (RMS) difference between the observed and model variable (eg, precipitation) field across the synoptic region. This matching is assessed on the GCM grid, and the analog days are selected from the observed record within 45 days of the day of the year of the model value being downscaled (e.g., *Hidalgo et al.* [2008]). So, for example, a model field of July 1 precipitation can only be matched to precipitation from observed analog days between May 18 and August 14, thereby ensuring that analogs are assigned from the correct season of the year.

Step 3. Find the one best matching analog day at the local scale

After this regional analog selection (step 2), the 30 analog days that most nearly match the model day being downscaled in the region about the point being downscaled (Fig. 2) have been identified. BCCA would at this point form a weighted average of the 30 analog days (selected over the entire domain in BCCA's case) for the final downscaled field, which leads to problems with drizzle and muted extremes. LOCA, in contrast, avoids these problems by instead selecting only *one* of the thirty analog days to be the final analog day used for downscaling at a point.

Because of the procedure outlined above, all 30 analog day values provide relatively good matches the model day value being downscaled at the synoptic-scale – that is, the wider region about the point being downscaled (e.g., the pink region illustrated in Fig. 2 for Seattle). However, each of the 30 analog days varies the quality of its match at the fine target grid locations. LOCA therefore picks the single one of the 30 analog days that offers the best match to the model day variable being downscaled in the immediate vicinity of the point being downscaled (ie, each grid cell).

To do this, bicubic interpolation is first used to interpolate the coarse grid model field and the coarsened observations of the 30 analog days to the fine grid resolution (1/16° here). Then, at each fine-resolution grid location, the single analog day from the pool of 30 analog days that minimizes the RMS difference between the interpolated model field and interpolated analog day in a square region of size ($2r+1$) fine-scale grid cells around the center of the grid point being downscaled is selected. *Pierce et al.* [2014] uses r = 10.

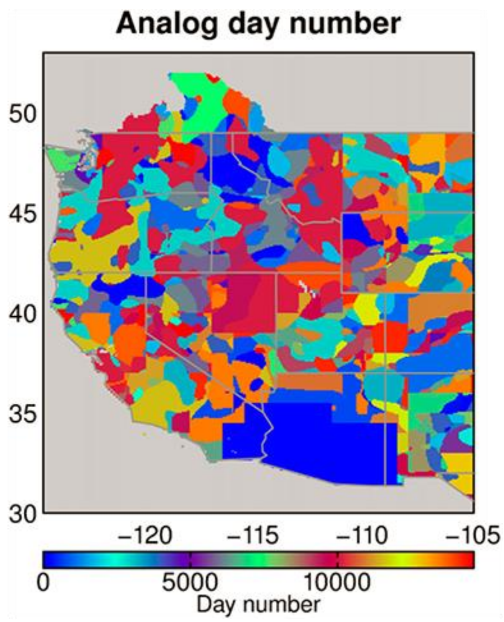

Figure 3. Example analog day number with integer day number starting 1 Jan 1970 and ending 31 Dec 2010. The GCM field being downscaled is precipitation on 1 Jan, 1950. This pattern is different for every model day being downscaled. *Source: Pierce et al.* [2014].

Since LOCA largely selects a different analog day at each fine grid location, the result is a jigsaw type pattern in the distribution of analog days (e.g., Figure 3). This pattern is not fixed in time, but rather changes for every model day being downscaled.

Step 4. Construct final downscaled field using scale factors

At the end of step 3, the final single analog day to use at a point has been identified. However the actual value found in the analog day is likely not identical to the value in the model day. In order to preserve the actual GCM values, the final selected analog day is scaled to match the original GCM value. For precipitation, the scale factor is the ratio between the interpolated fine-scale model field and the interpolated fine-scale analog day value. For temperature, the scale factor is the difference between the fine-scale model field and the interpolated fine-scale analog day value.

Finally, as shown in Figure 3, consideration should be given to account for subdomain edge effects to reduce spatial discontinuity in the downscaled fields. In LOCA, any point that is adjacent to a point that uses a different analog day for downscaling instead uses a linear combination of the originally selected analog day and the neighbor's analog day.

5.3.2 LOCA Bias Correction procedure

A description of the bias correction method (*Pierce et al.* [2015]) that was used in developing the daily high resolution (1/16° here) climate projections of precipitation, maximum (minimum) temperature is presented here.

The BCCA data product uses quantile mapping (QM) for bias correction. For example, given a model value to be bias corrected, the quantile of that value in the model's historical time period distribution is first computed, then the bias-corrected output value is the *observed* value at that quantile. One of the main reasons for developing a new bias correction for LOCA is that QM does not preserve the original GCM-predicted climate change signal in any given model (see, e.g., Maurer and Pierce, 2014). Roughly speaking, in locations that have synoptic time variability on the order of 5-20 days, QM tends to reduce the climate change signal; where synoptic variability is lower, QM increases the change signal. One of the design objectives for the LOCA bias correction was to do a better job preserving each model's original GCM-predicted climate change.

The bias correction proceeds in three steps that are described below: 1) Preconditioning is used to correct the annual cycle of daily values; 2) The distributions of values is corrected using the EDCDFm [*Li et al. 2010*] scheme for temperature or the Presrat [*Pierce et al. 2015*] scheme for precipitation; 3) A frequency-dependent bias correction (FDBC; *Pierce et al. 2015*) is applied to improve the final representation of variability as a function of time scale.

Preconditioning: Most bias correction schemes, including the ones used in BCSD, BCCA, and LOCA, consist of mapping from one CDF to another in various ways (see *Pierce et al. 2015* for a summary of these methods), often via QM. However, such mappings cannot alter the sequencing of the ranks of the values they are applied to (where rank 1 is the largest value in the time series, rank 2 is the second largest value, etc.). For example, bias correction might change the value seen on the hottest day in the model's time series from 43 C to 41 C, but it cannot change which day is the hottest day in the model's time series.

The foregoing implies that such methods cannot correct a misrepresentation of the annual cycle in the model's output, since that would appear as an error in the average ranks. For example, if in the observations August is climatologically the hottest month (rank 1) and July is the second hottest month (rank 2), but these are reversed in the model, then no CDF mapping technique that is applied to the entire time series will be able to fix this misrepresentation, since the ranks of the values are not altered.

To get around this problem, CDF mapping is typically applied in a restricted window of the model time series on the order of a month wide. For example, all July values might be bias corrected together, all August values bias corrected together, etc. (Sliding windows are also often used to avoid edge effects.) Although this works to correct the annual cycle, it leads to other problems since extreme phenomena are often not confined to a single month, but can occur at any time within a wider season. This leads to conflicting requirements, where a monthly or shorter window does the best job correcting the annual cycle, but a seasonal or longer window is best for correcting the extreme values. For example, California precipitation tends to be greatest in the winter; extreme precipitation days have occurred as early as November and as late as February. Similarly, extreme heat days in California have occurred as early as June and as late as September. Ideally all the "wet season precipitation extremes" and "hot season temperature extremes" should be bias corrected together, which would require a window size of at least 4 months. However using a 4-month wide BC window does a poor job correcting errors in the annual cycle (Pierce et al., 2015).

LOCA avoids this problem by doing a simple preconditioning step before the CDF mapping. The model's daily values are adjusted so that their daily means match the observed daily means, using an additive factor for temperature or multiplicative factor for precipitation. This preconditioning step rearranges the model's time series of rank values so that, on average, it matches the observations. In other words, it corrects the annual cycle, so that both the model and observations have the same hottest month, the same second-hottest month, etc. This allows a wide (seasonal) window to be used in the next step, where the CDF mapping is applied.

EDCDFm and Presrat: The CDF mapping technique used in LOCA is EDCDFm for temperature and Presrat for precipitation. They are conceptually similar techniques, although they differ in details. Each is equivalent to simple quantile mapping over the historical era. For future periods, EDCDFm constructs the bias-corrected CDF as the observed historical CDF *plus* the model-predicted future change computed at each quantile. In other words, the target CDF for the future conditions becomes the historical CDF added quantile-by-quantile to the CDF of future model changes. Presrat is similar, but constructs the bias-corrected CDF as the observed historical CDF *times* the model-predicted factor by which values at that quantile change in the future. Presrat also multiplies by a factor calculated to ensure that the future bias-corrected change in mean value matches the original model's predicted change in mean value, and applies a zero-precipitation threshold so that over the historical period, the number of zero-precipitation days in the model matches that observed. The CDF mapping is applied iteratively in three windows that are 91, 181, and 365 days wide, respectively.

Frequency-dependent bias correction (FDBC): The frequency-dependent bias correction or FDBC is described in *Pierce et al.* [2015]. *Pierce et al.* [2015] show that using bias correction methods such as quantile mapping and cumulative distribution function transform can significantly alter the GCM's mean climate change signal and alter the spectra of the time series to which they are applied in an unintended fashion. A larger issue, however, is that GCMs are often limited in their ability to simulate variance across the frequency spectrum, meaning that their sequencing of variations at different time resolutions, from daily to decadal, may be substantially unrealistic compared to observed sequencing. Many applications of climate information, such as water resources management, are highly sensitive to variations in climate sequences (e.g. wet and dry periods, storm characteristics). This GCM deficiency motivated the development of the FDBC approach, which uses a digital filter in the frequency domain to adjust the amplitudes of the model variability in different frequency bands to better match the observations. Use of a frequency-based bias correction approach coupled with the LOCA spatial downscaling procedure is one means of preserving daily extremes and variability as they have appeared in the observational record in the final downscaled GCM data product.

For each grid cell, normalized time series spectra are developed both for the GCM data and the aggregated *Livneh et al.* [2015] observed data covering periods from 2 days to 11 years in 100 logarithmically-spaced frequency bands. The GCM spectra are bias corrected as a ratio using the observed spectra, and converted back to a time series.

5.3.3 The common 1x1 degree grid

The entire downscaling process – GCM bias correction, then spatial disaggregation with LOCA – is repeated twice to produce the final 1/16th degree LOCA product: once for downscaling from the original coarse resolution GCM grid to a common 1x1 degree grid, and then again to downscale from the common 1x1 degree grid to the 1/16th degree grid. This approach is taken because different GCMs generally have different coarse resolutions, which can range from 1x1 degrees or finer to 2.8x2.8 degrees. If only one iteration of LOCA were used, going directly from the GCM native grid to the 1/16th degree grid, then the models would be bias corrected only on their coarse resolution grids, which differ significantly across the different models. At worst, the coarsest resolution GCMs would be bias corrected using only 1/8th the information used to bias correct the finest resolution GCMs. This would introduce significant disparities across the models.

The solution chosen here is to use the two-step process, so that all models are bias corrected on the same 1x1 degree grid before downscaling to 1/16th degree, and so receive the same observed information in the bias correction step. The more complicated two-step application of LOCA was used in preference to a simple interpolation from the coarse model grid to the 1x1 degree common grid because tests indicated that interpolation increased the spatial coherence of the modeled precipitation field, which is detrimental to the realism of runoff simulations that are driven primarily by the downscaled precipitation fields.

As a last step, the 1/16° GCM projections are adjusted using a ratio for precipitation and difference for temperature such that their monthly means match-up with the fine-scale observations over the observed period. This step is required for technical reasons arising out of how LOCA handles climatology over the historical period. For future periods, the adjustments are chosen to maintain the property that the original GCM-predicted climate change signal is preserved.

5.3.4 Model Calendars

The various GCMs supply data on a variety of different calendars, so before the LOCA downscaling procedure was applied, the model data were interpolated to the common civil (standard) calendar. Most models use a non-leap year calendar, where leap days are omitted. In this case, leap days were constructed as needed by linear interpolation between the model's values on Feb 28 and Mar 1. Since this affects only one day every four years, the overall impact of this interpolation on the final results of impact studies is likely to be small.

A more significant problem is posed by the Hadley center models (HadGEM2-CC, HadGEM2-AO, and HadGEM2-ES here), which tend to use a 360-day per year calendar. In this case 5 days per year need to be added in non-leap years, and 6 days per year for leap years, to produce model data on a standard calendar. Rather than picking fixed days-of-the-year for interpolation, which might lead to discernable artifacts on those days, for each year a day was randomly selected from each 1/5th of the year to be inserted via interpolation. Leap days were always inserted on Feb 29, however.

The list of days inserted is available for all models, so that users who are concerned that this procedure might affect their results can omit all interpolated days, at the cost of having to work with data on a variety of different calendars.

5.4 Bias correction with spatial disaggregation (BCSDm)

The basic steps of the BCSDm procedure to develop daily precipitation and temperature fields are described below, for complete details refer to, *Bureau of Reclamation* [2013].

1. As the first step, all GCMs are re-gridded from their native scale to a 1º (latitude) $\times$1º (longitude) grid using bilinear interpolation. Fine grid (1/8º [latitude] $\times$ 1/8º [longitude]) observations [*Maurer et al.*, 2002] are also gridded to the same 1º$\times$1º resolution.
2. Using the gridded 1º$\times$1º GCM data, monthly biases in the GCMs are corrected using the coarsened observation grid, and applying quantile mapping on a grid cell by grid cell basis. This generates the bias-corrected GCM outputs at the coarse grid resolution of 1º$\times$1º.
3. Next, the bias-corrected GCM outputs are spatially disaggregated to the fine grid resolution of 1/8º (latitude) $\times$1/8º (longitude) using bilinear interpolation.
4. An anomaly field is computed as the difference between the fine grid observations (1/8º$\times$1/8º) and the coarsened (1º$\times$1º) observations which are subsequently re-interpolated to the fine grid resolution of 1/8º $\times$1/8º. Anomalies are computed as a ratio for precipitation, and as a difference for temperature.
5. The anomaly field (step 4) is then applied to the bias corrected GCM outputs (step 3) to derive the final set of monthly bias-corrected GCM outputs at the fine grid resolution (1/8º$\times$1/8º).
6. The fine resolution gridded monthly GCM values are subsequently disaggregated to daily fine resolution gridded values by selecting a historical month from the fine grid observations and then scaling it to match the monthly value at the respective grid cells. The historical month is selected based on the similarity of monthly precipitation total only; i.e., no temperature information is used in the month selection.

5.5 Bias correction with constructed analogs (BCCA)

The basic steps of the BCCA procedure are described below, for complete details see *Maurer et al.*[2010] and for a summary, refer to *Gutmann et al.* [2014].

1. Correct daily biases in the coarse model grid using quantile mapping from the coarsened observation grid.
2. Select 30 analog days from the entire grid of coarsened observations that have the best match with model data on a given day. The matches are evaluated over the entire domain being downscaled.
3. Compute the optimal weights needed such that a weighted linear combination of the 30 analog days has the best match with the model data over the entire domain.
4. Apply the same optimal weights to the fine observations from the same 30 analog days to obtain a downscaled field.

6 Methodology

Three variables were examined: daily precipitation (*P*, mm), minimum daily temperature (T_{min}, ºC) and maximum daily temperature (T_{max}, ºC). For each variable, statistics were computed for a **historical period** (1970-1999), **future period** (2040-2069) and the difference between historical and future periods denoting future change. Future periods are denoted as either “rcp45” for RCP 4.5 model runs (Appendix A), “rcp85” for RCP 8.5 scenarios (Appendix B) and “all projections” for a collection of both RCP 4.5 and RCP 8.5 projections (Section 7). The calculated statistics include:

1. **Mean daily:** Mean over the historical or future period of daily values.
2. **Max daily:** Maximum over the historical or future period of daily values.
3. **Mean monthly (daily value):** Mean daily value by month over the historical or future period.

6.1 Difference maps

Three types of difference maps are computed:

1. Differences between average observed datasets over the historical period.
2. Differences between historical and future averages for each downscaling method. These difference maps show where climate projections are indicating increases or decreases.
3. Differences between the historical and future period averages for the difference between each method, eg. ($LOCA_{future}$-$LOCA_{historical}$) - ($BCSDm_{future}$-$BCSDm_{historical}$). These indicate relative changes between the two methods. For example, a positive difference between LOCA-BCSDm during the historical and future period would indicate LOCA produces a greater future change relative to BCSDm.

6.2 Monthly basin average comparisons

For the monthly data, five HUC4 basins were chosen within selected HUC2s in the west, and basin averages were computed for each projection over the historical and future period. Figure 4 shows the HUC4 basins used (in black) with the encompassing HUC2 (in grey). These are displayed as boxplots with color indicating the month of the year and the spread showing the range from models. Differences between models is also shown in the monthly case, the interpretation is the same as described in the previous section.

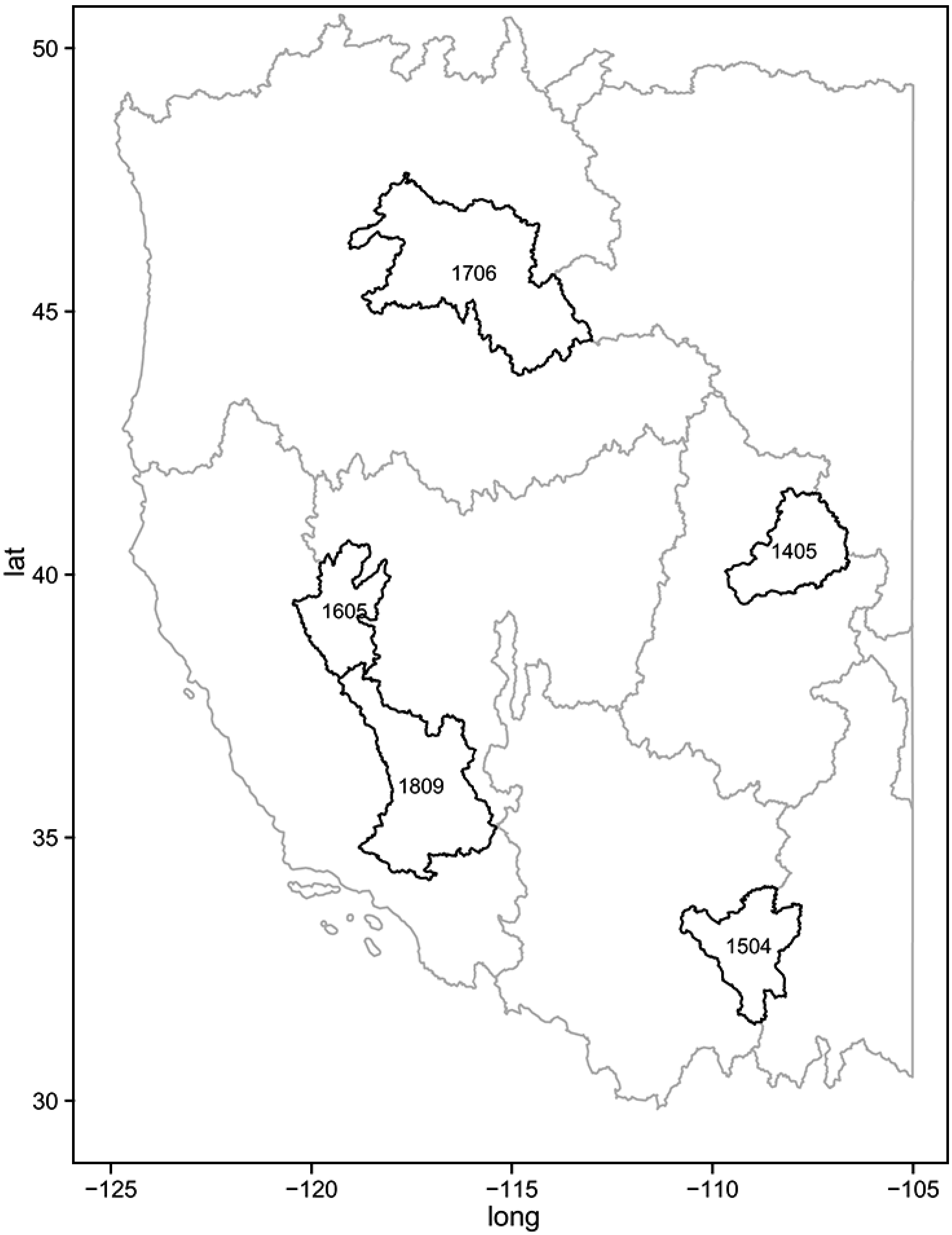

Figure 4: HUC4 basins used in monthly basin average statistics; where, 1405 is the White-Yampa; 1504 is the Upper Gila; 1605 is the Central Lahontan; 1706 is the Lower Snake; 1809 is the Northern Mojave-Mono Lake.

6.3 Common Models

Statistics were computed for 18 CMIP5 models which were common to all three downscaling methods. The models are listed in Table 2. For each model a single RCP 4.5 and RCP 8.5 projection was used. Combining both RCP 4.5 and RCP 8.5 provides an ensemble of 36 members. This ensemble is assumed to be a representative sample of the larger CMIP5 ensemble.

Table 2: CMIP5 Models included in this report

CMIP5 Climate Modeling Group1	CMIP5 Climate Model ID
Commonwealth Scientific and Industrial Research Organization and Bureau of Meteorology, Australia	ACCESS1-0
Beijing Climate Center, China Meteorological Administration	BCC-CSM1-1
Canadian Centre for Climate Modelling and Analysis	CanESM2
Community Earth System Model Contributors	CESM1-BGC
Centre National de Recherches Météorologiques/ Centre Européen de Recherche et Formation Avancée en Calcul Scientifique	CNRM-CM5
Commonwealth Scientific and Industrial Research Organization, Queensland Climate Change Centre of Excellence	CSIRO-Mk3-6-0
NOAA Geophysical Fluid Dynamics Laboratory	GFDL-CM3 GFDL-ESM2G GFDL-ESM2M
Institute for Numerical Mathematics	INM-CM4
Institut Pierre-Simon Laplace	IPSL-CM5A-MR
Japan Agency for Marine-Earth Science and Technology, Atmosphere and Ocean Research Institute (The University of Tokyo), and National Institute for Environmental Studies	MIROC-ESM MIROC-ESM CHEM
Atmosphere and Ocean Research Institute (The University of Tokyo), National Institute for Environmental Studies, and Japan Agency for Marine-Earth Science and Technology	MIROC5
Max-Planck-Institut für Meteorologie (Max Planck Institute for Meteorology)	MPI-ESM-LR MPI-ESM-MR
Meteorological Research Institute	MRI-CGCM3
Norwegian Climate Centre	NorESM1-M

6.4 Historical Observational datasets

All the downscaling methods described above require a gridded observation dataset for calibration and to determine the fine grid resolution. The BCCA and BCSDm use the *Maurer et al.* [2002] dataset which is at 1/8º grid resolution. LOCA uses the *Livneh et al.* [2015] dataset which is at 1⁄16º grid resolution. To perform the comparison, the *Livneh et al.* [2015] dataset was aggregated to the 1/8º *Maurer et al.* [2002] grid resolution. Both the *Livneh et al.* [2015] and the *Maurer et al.* [2002] data are based on the same underlying procedure so minimal differences are expected. To illustrate the differences between these two datasets, comparisons are shown for both annual mean and annual max over the historical period for precipitation (Figures 5 and 6), T_{max} (Figures 7 and 8) and T_{min} (Figure 9). Note that some differences are large but these typically fall outside of the CONUS boundaries.

The three major differences in the Maurer and Livneh data sets are: (i) spatial resolution, with the former coarser than the latter, which is expected to modestly influence the gridding results particularly in areas of topographical complexity, (ii) The station data are similar but not identical over CONUS, which would produce isolated 'hot spots',i.e. localized differences, while Livneh used a larger set of stations over Canada, and a much larger set of station data over Mexico that result in larger differences, and (iii) for precipitation, both data sets are scaled to match long-term, 30-year climatological precipitation products that are 'orographically aware', such as the PRISM (*Daly et al.* [1997]) product over CONUS that assume greater precipitation with increasing elevation. However, over CONUS Maurer data are scaled to the 1961-1990 PRISM climatology, whereas *Livneh et al.* [2015] is scaled to the 1981-2010 PRISM climatology. More importantly, over Mexico and Canada (Columbia R. headwaters notwithstanding), the Maurer data are un-scaled, whereas the Livneh data have been scaled to a *Vose et al.* [2014] 1981-2010 climatology, which would produce large differences.

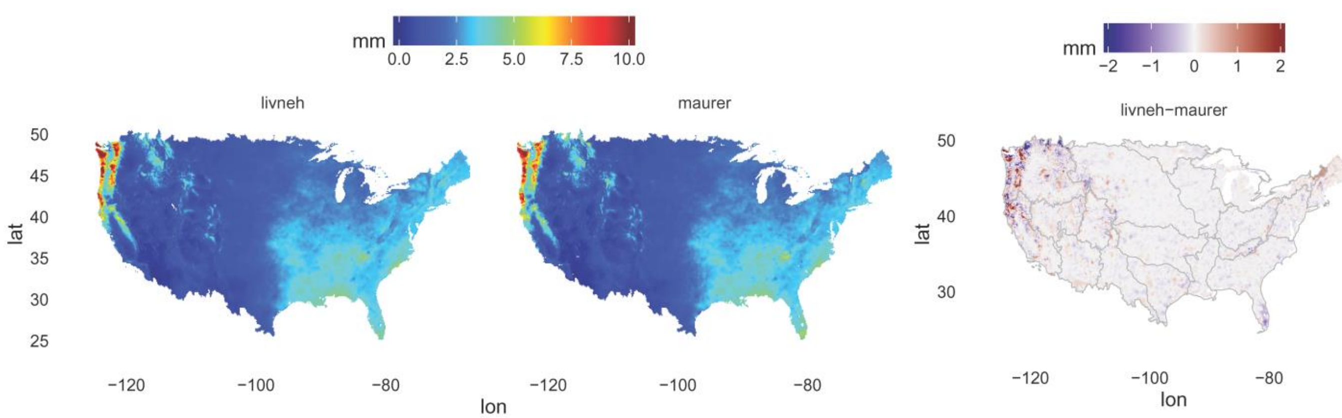

Figure 5: Mean daily precipitation from 1970-1999 for the Livneh dataset (left), the Maurer dataset (middle) and the difference (right).

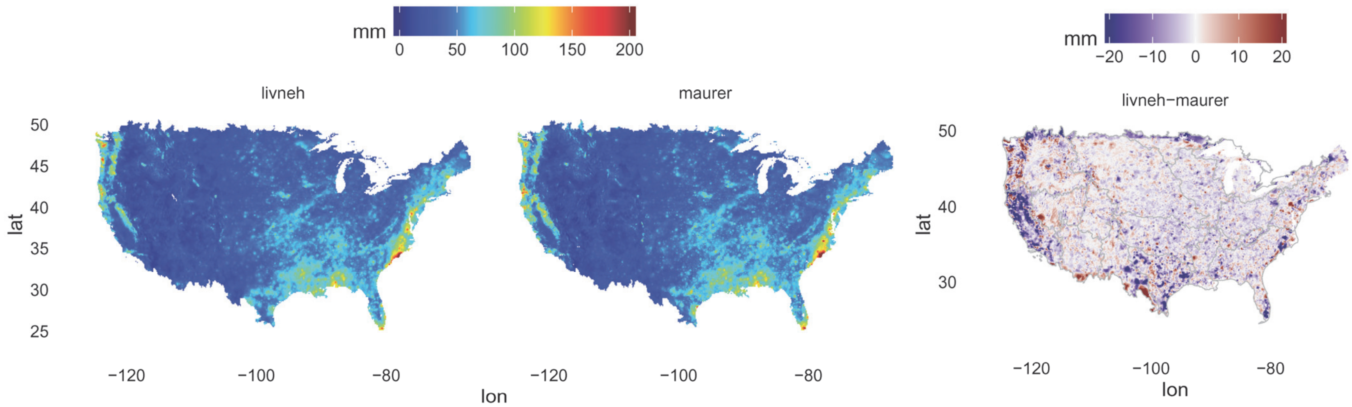

Figure 6: Max daily precipitation from 1970-1999 for the Livneh dataset (left), the Maurer dataset (middle) and the difference (right).

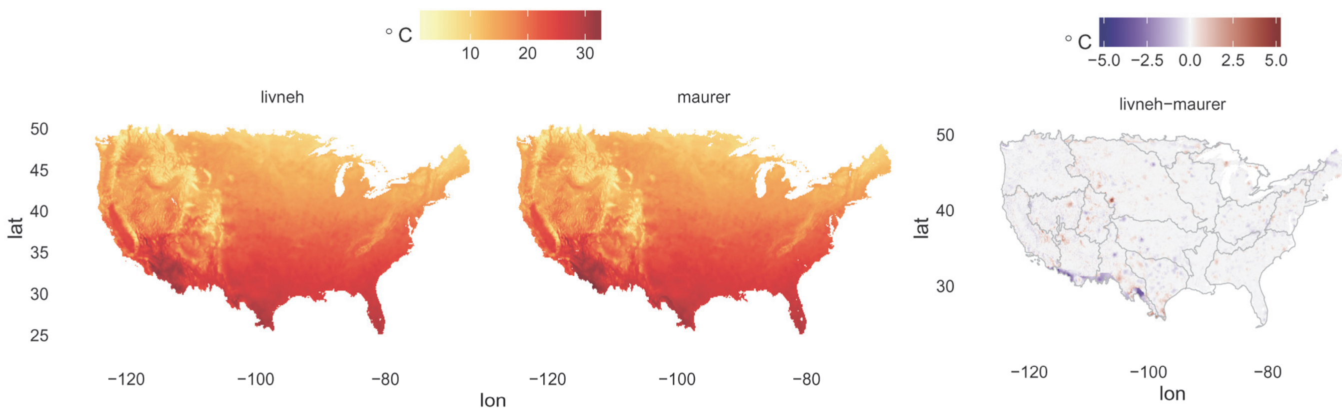

Figure 7: Mean daily T_{max} from 1970-1999 for the Livneh dataset (left), the Maurer dataset (middle) and the difference (right).

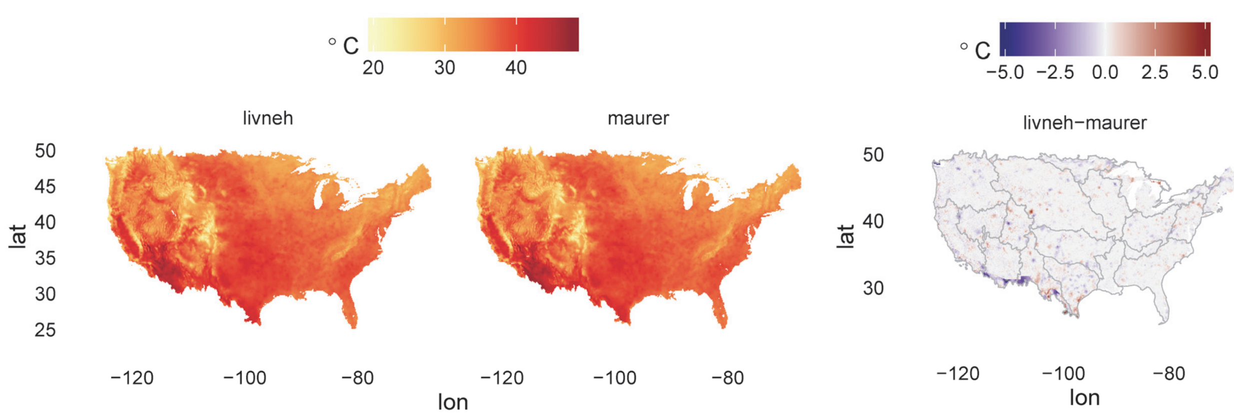

Figure 8: Period max daily T_{max} from 1970-1999 for the Livneh dataset (left), the Maurer dataset (middle) and the difference (right).

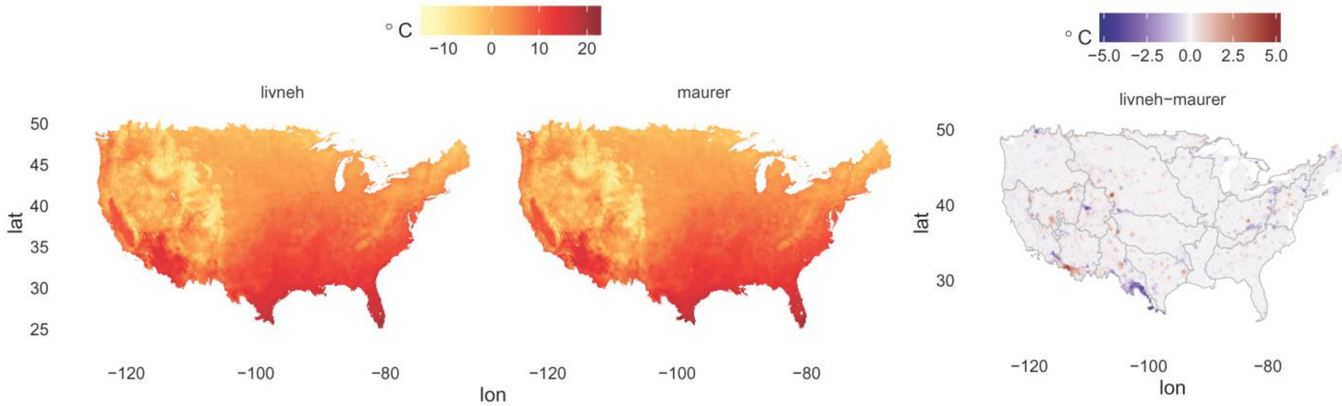

Figure 9: Mean daily T_{min} from 1970-1999 for the Livneh dataset (left), the Maurer dataset (middle) and the difference (right).

7 Results

The results present 2 main types of graphics for 3 variables and 3 sets of projections, totaling 24 figures. Results are shown for both RCP 4.5 and RCP 8.5 projections in figures 10-17. See Appendices A and B for RCP 4.5 and RCP 8.5 specific figures. The statistics used in the figures are described in general in Section 6. Figures of the annual spatial distribution of precipitation, T_{max}, T_{min}, are followed by monthly boxplot figures for each variable in the same order.

Figure 10 shows the grid cell-wise ensemble median of mean daily precipitation for the historical period (left column) and the future period (second column), using both RCP 4.5 and 8.5 projections and the difference (third column). For the first three columns, rows correspond to each method: BCCA (top), BCSDm (middle) and LOCA (bottom). The fourth column show differences between future changes of each method. The rows in the fourth column represent differences between pairs of methods, LOCA-BCSDm (top row), LOCA-BCCA (middle row) and BCSDm-BCCA (bottom row). The HUC2 basins are superimposed on the difference maps to provide a reference for particular basins of interest. For the mean daily precipitation difference between future and historical periods, all methods show general agreement in terms of spatial patterns. Comparing the difference maps in the fourth column, LOCA is generally drier than BCSDm except in the Rio Grande, and Texas-Gulf regions. This difference between LOCA and BCCA is somewhat less pronounced but point towards similar findings with BCSDm. The difference between BCSDm and BCCA shows that the BCSDm is somewhat wetter for the eastern U.S. basins.

Figure 11 is for the ensemble median of max daily precipitation. The descriptions are the same as above. BCCA tends to produce somewhat lower max daily precipitation than LOCA or BCSDm. LOCA tends to produce greater increases in maxima in the southeast relative to the other methods.

Figures 12 and 13 are the same as Figures 10 and 11 respectively, but for T_{max}. All methods show general agreement in terms of spatial patterns and all indicate an increase in mean daily T_{max} but can disagree by as much as 1ºC on the magnitude of future change. BCCA tends to show regional biases in mean daily T_{max} relative to LOCA and BCSDm, with the latter methods in somewhat closer agreement (Figure 12).

Figure 14 is the same as Figure 11 but for T_{min}. The interpretations are similar to those in the previous paragraph for T_{max}.

Figure 15 shows boxplots of mean monthly (daily value) basin average precipitation for 5 HUC4s, one in each of the westernmost HUC2s. Each boxplot represents the spread of all ensemble members, with the color indicating the month for the historical period (first column), the future period (second column) and the difference (third column). The methods are shown in each row: BCCA (top row), BCSDm (middle row) and LOCA (bottom row). In this view there is practically no change in future precipitation on average over these basins. The rows in the fourth column represent differences between pairs of methods, LOCA-BCSDm (top row), LOCA-BCCA (middle row) and BCSDm-BCCA (bottom row). Again, the difference in precipitation magnitude is practically negligible across the methods.

Figures 16 is the same as Figure 15 but for T_{max}. All methods generally indicate an increase in mean monthly (daily value) basin average T_{max}. BCSDm tends to produce lower mean monthly (daily value) basin average T_{max} than LOCA or BCCA. Figures 17 is the same as Figure 15, but for T_{min}. All methods generally indicate an increase in mean monthly (daily value) basin average T_{min} and practically show no bias relative to each other.

8 Conclusions

This report provides an overview and comparisons of three downscaling methods: BCCA, BCSDm and LOCA. The analysis conducted for this report was intended to present some salient features of these three datasets but not intended to be an exhaustive evaluation or comparison. For a more comprehensive comparison see *Maurer et al.* [2010], *Pierce et al.* [2014] and [*Gutmann et al.*, 2014]. At the level of aggregation presented here, LOCA and BCSDm perform comparably as shown in the maps, but at the monthly time scale the box plots show a low bias in T_{max} compared to both LOCA and BCCA.

9 References

Bureau of Reclamation, Downscaled CMIP3 and CMIP5 Climate and Hydrology Projections, *Tech rep.*, 2013.

Daly, C., Taylor, G. H., & Gibson, W. P. The PRISM approach to mapping precipitation and temperature. In *Proc., 10th AMS Conf. on Applied Climatology* (pp. 20-23) (1997).

Gutmann, E., T. Pruitt, M. P. Clark, L. Brekke, J. R. Arnold, D. A. Raff, and R. M. Rasmussen, An intercomparison of statistical downscaling methods used for water resource assessments in the United States, *Water Resources Research 50, 50*(9), 7167–7186, 2014.

Hidalgo, H.G., M. D. Dettinger, and D. R. Cayan, Downscaling with constructed analogues: Daily precipitation and temperature fields over the United States. *CEC PIER Project Report,* CEC-500-2007-123, 48 pp, 2008.

Livneh, B., E. A. Rosenberg, C. Lin, B. Nijssen, V. Mishra, K. M. Andreadis, E. P. Maurer, and D. P. Lettenmaier, A Long-Term Hydrologically Based Dataset of Land Surface Fluxes and States for the Conterminous United States: Update and Extensions*, *Journal of Climate, 26* (23), 9384-9392, 2013.

Livneh B., T.J. Bohn, D.S. Pierce, F. Munoz-Ariola, B. Nijssen, R. Vose, D. Cayan, and L.D. Brekke, A spatially comprehensive, hydrometeorological data set for Mexico, the U.S., and southern Canada 1950-2013, *Nature Scientific Data*, 2, 150042, doi:10.1038/sdata.2015.42, 2015.

Maurer, E. P., A. W. Wood, J. C. Adam, D. P. Lettenmaier, and B. Nijssen, A Long-Term Hydrologically Based Dataset of Land Surface Fluxes and States for the Conterminous United States, *Journal of Climate*, *15*(22), 3237-3251, 2002.

Maurer, E. P., H. G. Hidalgo, T. Das, M. D. Dettinger, and D. R. Cayan, The utility of daily large-scale climate data in the assessment of climate change impacts on daily stream flow in California, *Hydrology and Earth System Sciences, 14*(6), 1125-1138, 2010.

Pierce, D. W., D. R. Cayan, and B. L. Thrasher, Statistical Downscaling Using Localized Constructed Analogs (LOCA), *Journal of Hydrometeorology, 15*(6), 2558-2585, 2014.

Pierce, D. D. R. Cayan, E. P. Maurer, J. T. Abatzoglou, and K. Hegewisch, Improved Bias Correction Techniques for Hydrological Simulations of Climate Change, *Journal of Hydrometeorology, 16*(6), 2421-2442, 2015.

Thrasher, B., E. P. Maurer, C. McKellar, and P. B. Duffy, Technical Note: Bias correcting climate model simulated daily temperature extremes with quantile mapping, *Hydrology and Earth System Sciences*, *16*(9), 3309-3314, 2014.

Vose, R. S., et al. Improved historical temperature and precipitation time series for US climate divisions. *Journal of Applied Meteorology and Climatology*, 53(5), 1232-1251 (2014).

Wood, A., L. Leung, V. Sridhar, and D. Lettenmeir, Hydrologic implications of dynamical and statistical approaches to downscaling climate model outputs, *Climate Change, 15*(62), 189-216, 2004.

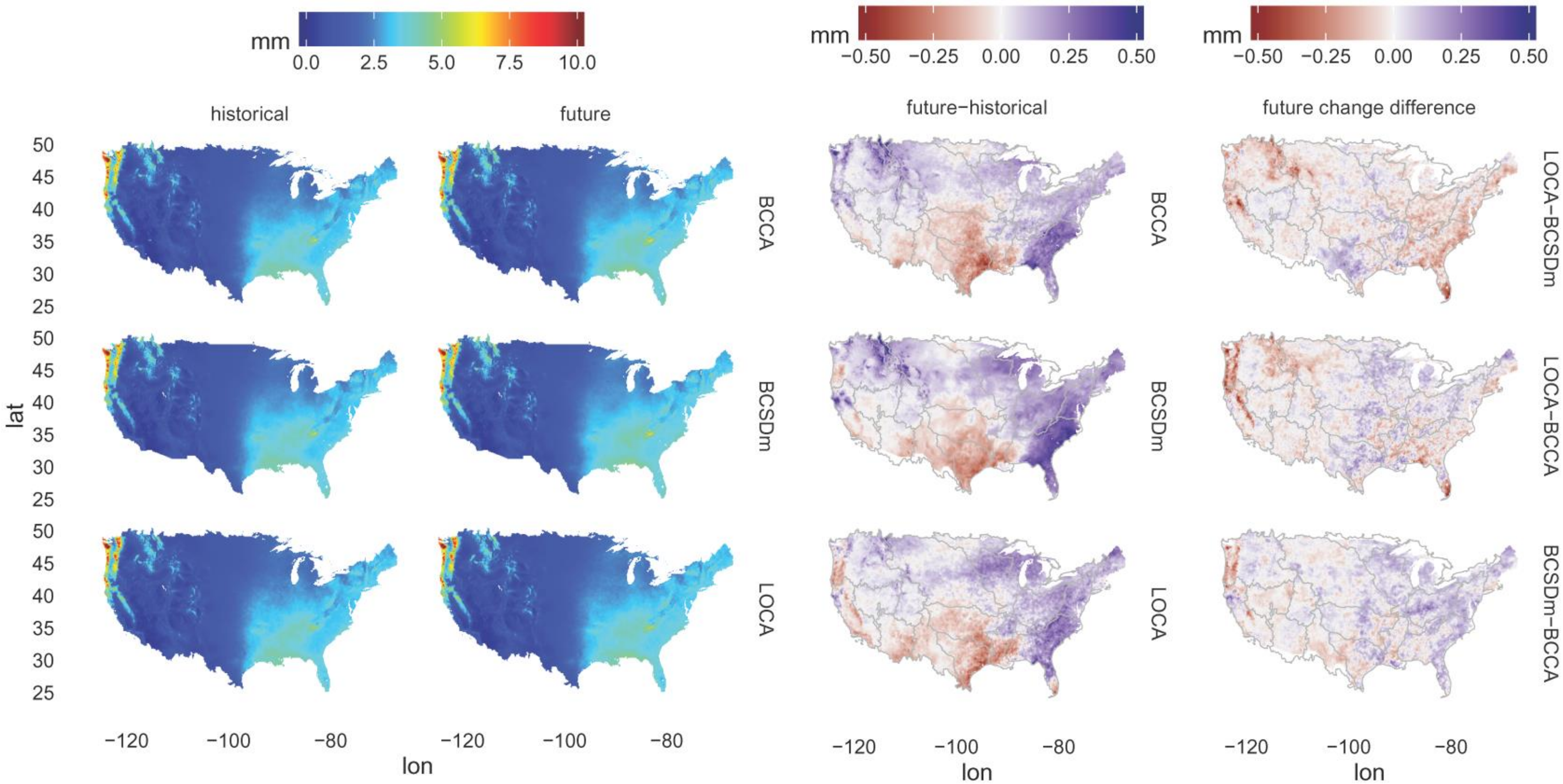

Figure 10: Ensemble median of mean daily precipitation for the historical period (1970-1999, first column), the future period (2040-2069, second column), using both RCP 4.5 and RCP 8.5 and the difference (third column). Rows correspond to each method: BCCA (top), BCSDm (middle) and LOCA (bottom). The fourth column show differences between future changes of each method. The rows in the fourth column represent differences between pairs of methods, LOCA-BCSDm (top row), LOCA-BCCA (middle row) and BCSDm-BCCA (bottom row).

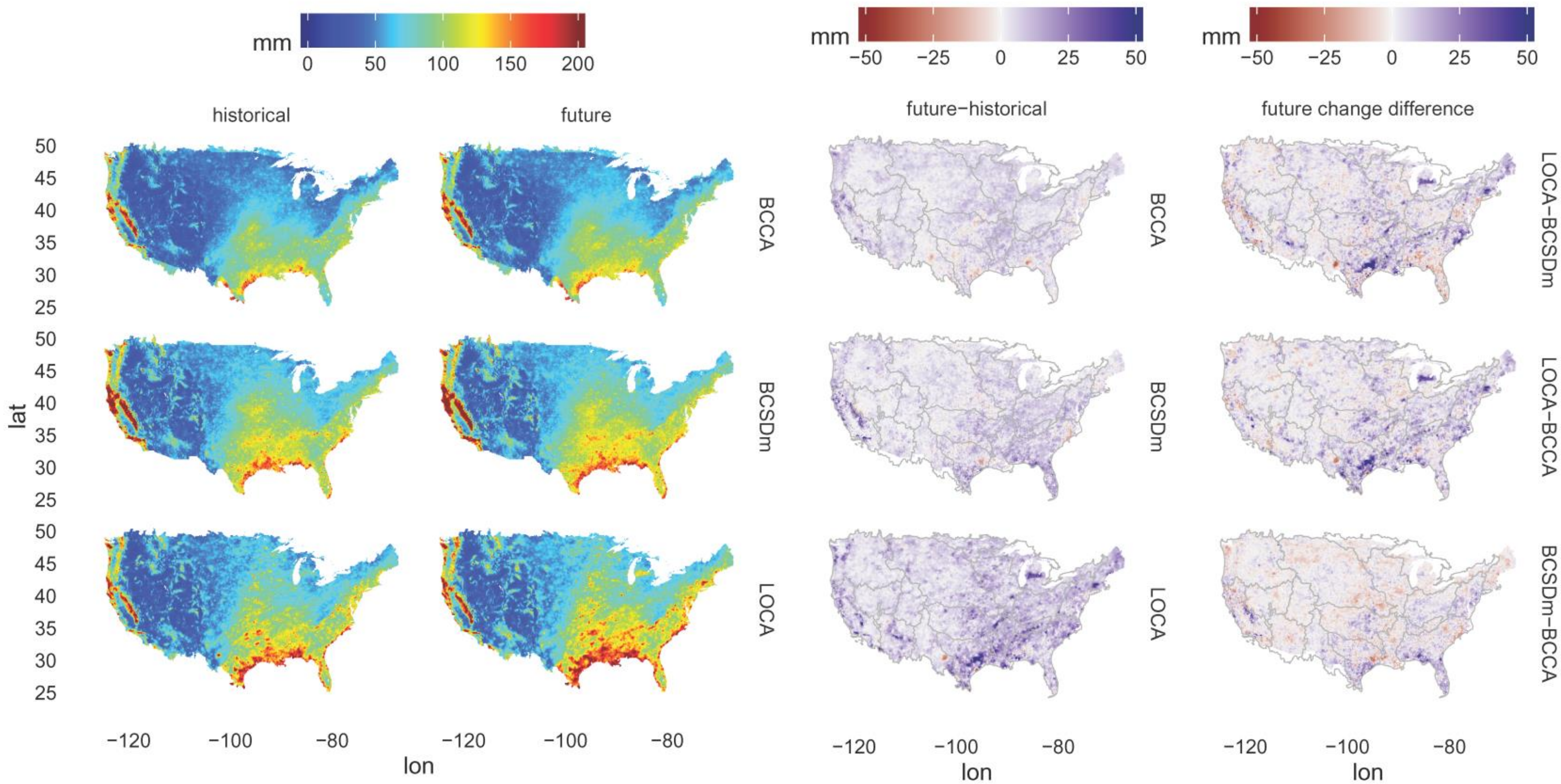

Figure 11: Ensemble median of max daily precipitation for the historical period (1970-1999, first column), the future period (2040-2069, second column) using both RCP 4.5 and RCP 8.5 and the difference (third column). Rows correspond to each method: BCCA (top), BCSDm (middle) and LOCA (bottom). The fourth column show differences between future changes of each method. The rows in the fourth column represent differences between pairs of methods, LOCA-BCSDm (top row), LOCA-BCCA (middle row) and BCSDm-BCCA (bottom row).

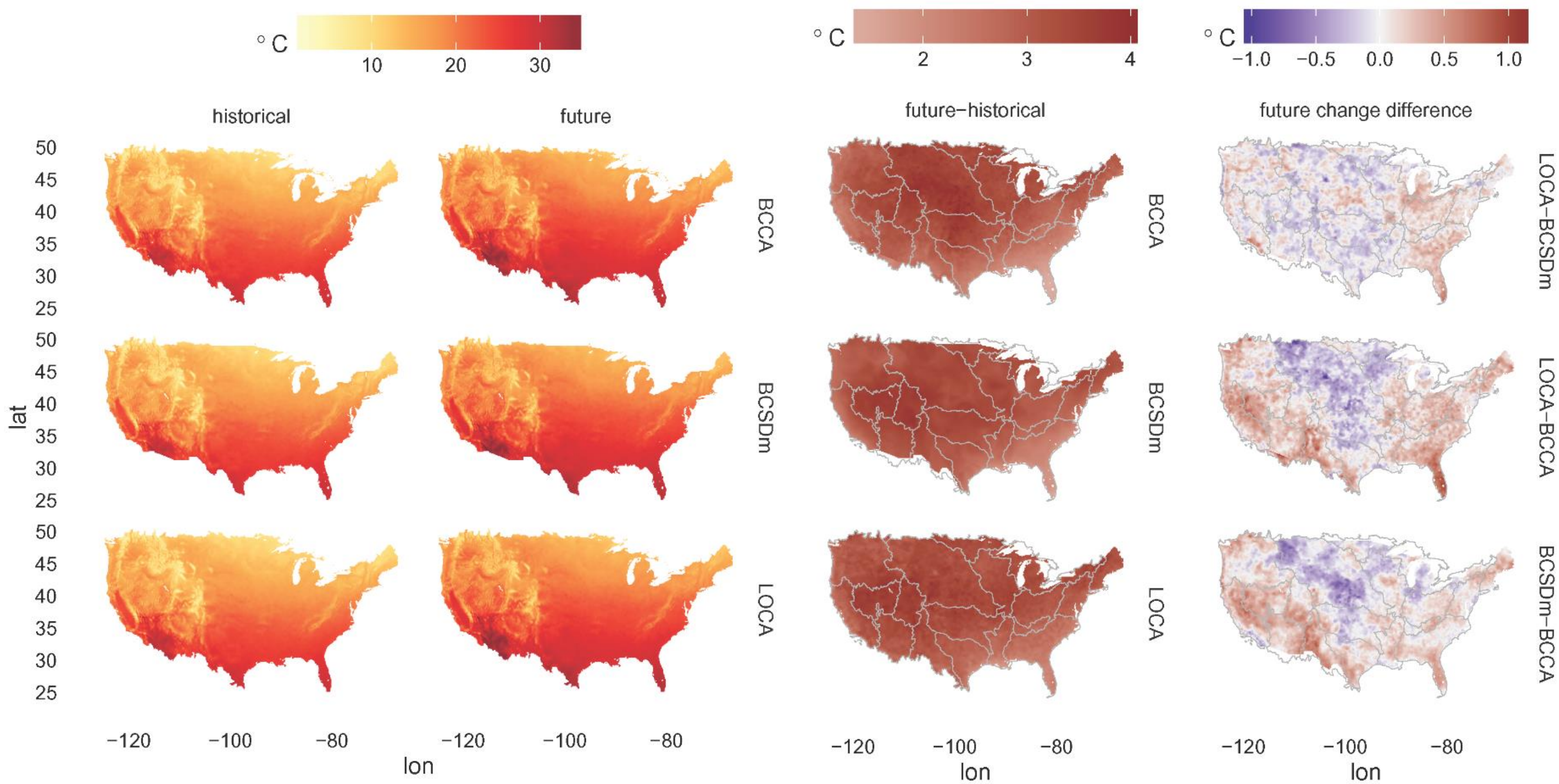

Figure 12: Ensemble median of mean daily T_{max} for the historical period (1970-1999, first column), the future period (2040-2069, second column) using both RCP 4.5 and RCP 8.5 and the difference (third column). Rows correspond to each method: BCCA (top), BCSDm (middle) and LOCA (bottom). The fourth column show differences between future changes of each method. The rows in the fourth column represent differences between pairs of methods, LOCA-BCSDm (top row), LOCA-BCCA (middle row) and BCSDm-BCCA (bottom row).

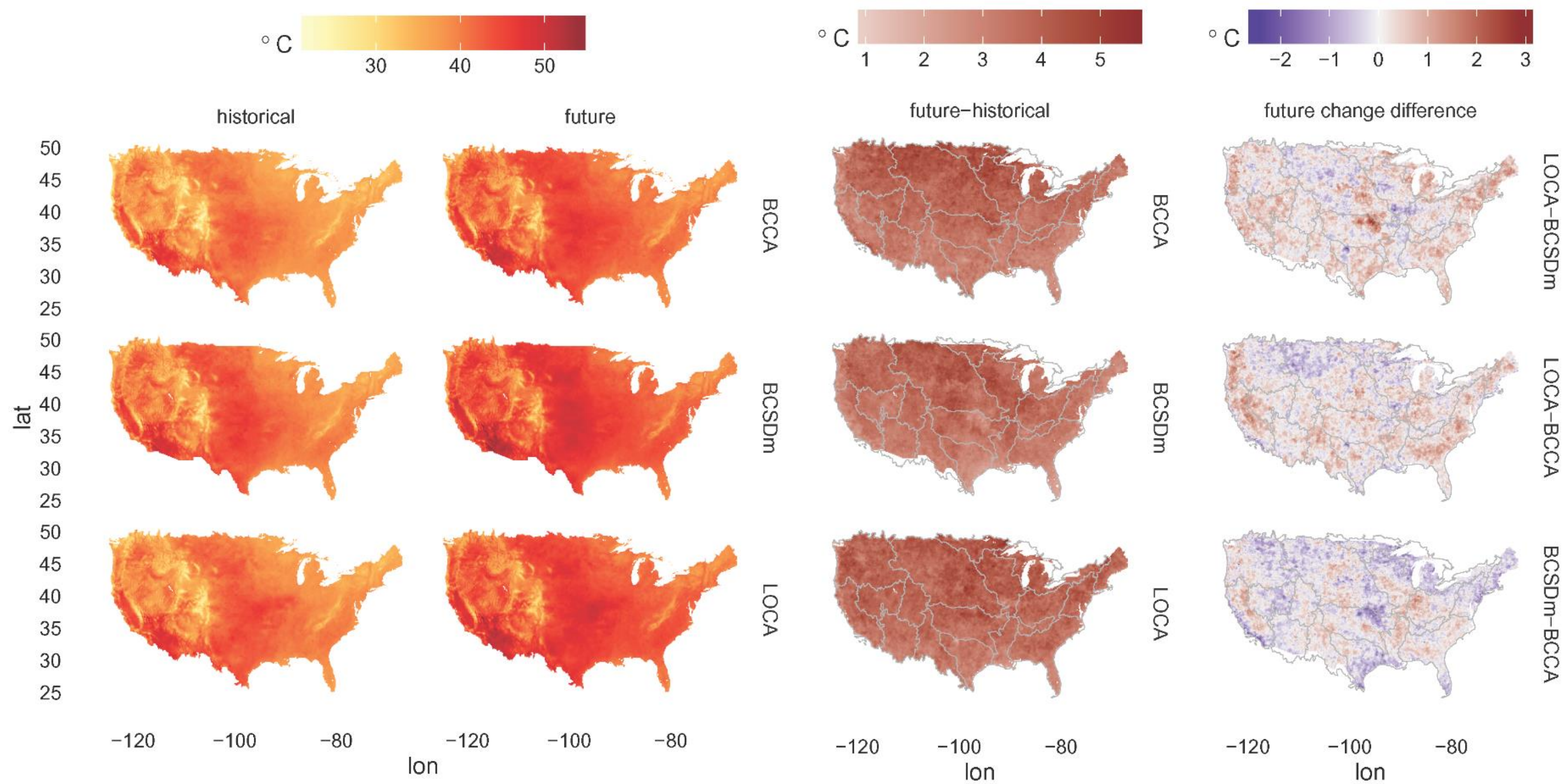

Figure 13: Ensemble median of max daily T_{max} for the historical period (1970-1999, first column), the future period (2040-2069, second column) using both RCP 4.5 and RCP 8.5 and the difference (third column). Rows correspond to each method: BCCA (top), BCSDm (middle) and LOCA (bottom). The fourth column show differences between future changes of each method. The rows in the fourth column represent differences between pairs of methods, LOCA-BCSDm (top row), LOCA-BCCA (middle row) and BCSDm-BCCA (bottom row).

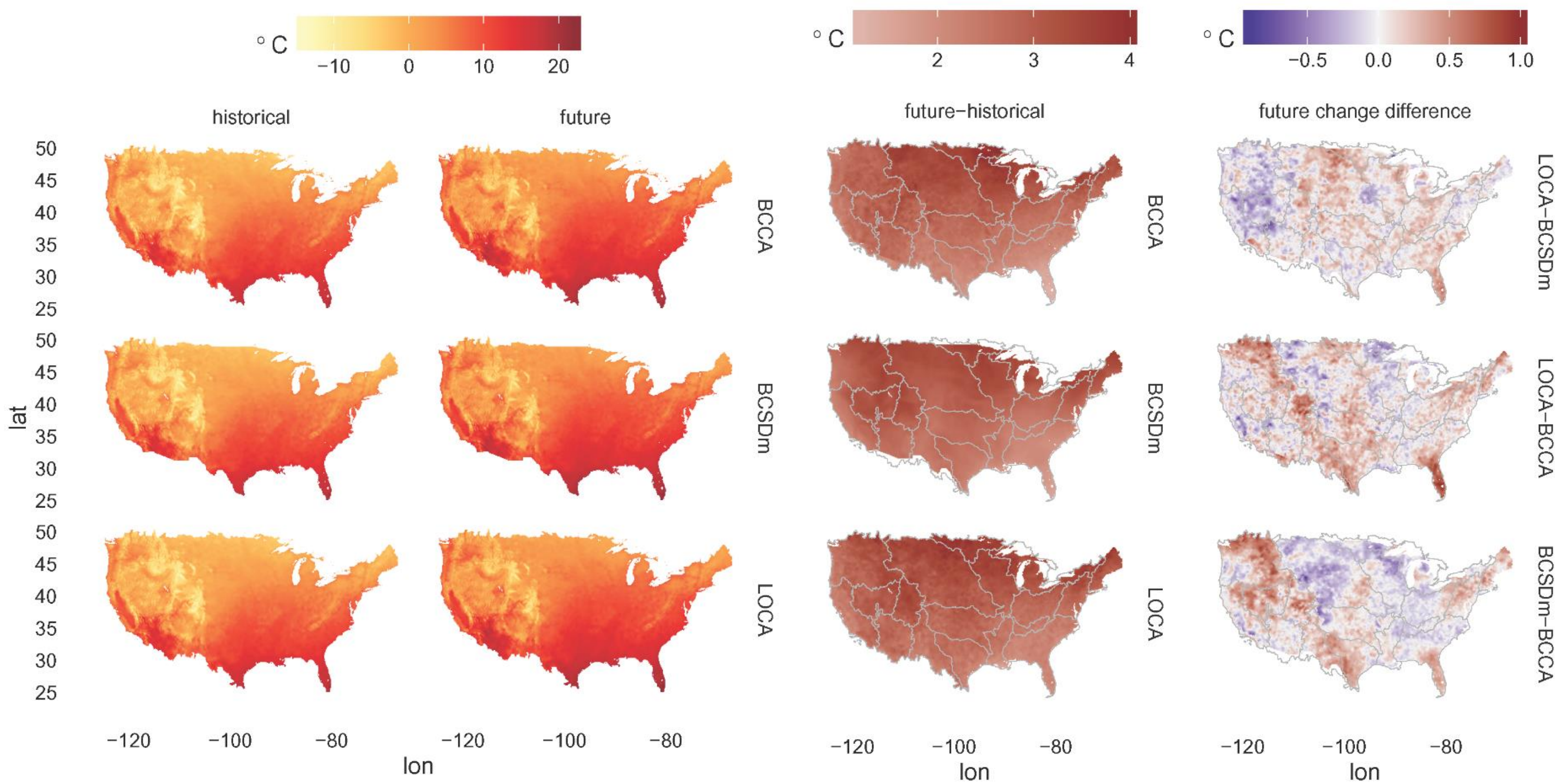

Figure 14: Ensemble median of mean daily T_{min} for the historical period (1970-1999, first column), the future period (2040-2069, second column) using both RCP 4.5 and RCP 8.5 and the difference (third column). Rows correspond to each method: BCCA (top), BCSDm (middle) and LOCA (bottom). The fourth column show differences between future changes of each method. The rows in the fourth column represent differences between pairs of methods, LOCA-BCSDm (top row), LOCA-BCCA (middle row) and BCSDm-BCCA (bottom row).

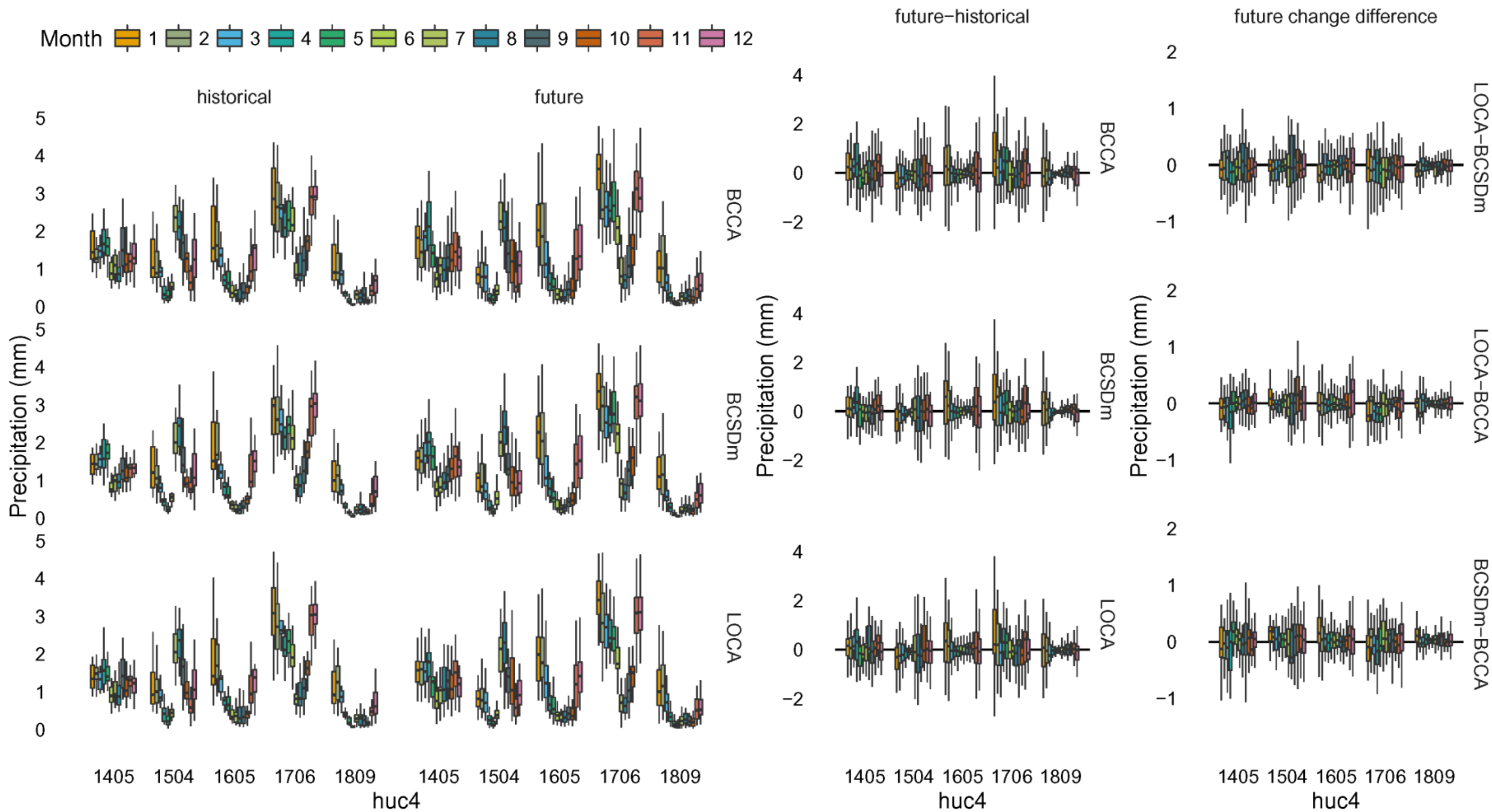

Figure 15: Boxplots of mean monthly (daily value) basin average precipitation for 5 HUC4s, one in each of the westernmost HUC2s. Each boxplot represents the spread of all ensemble members, with the color indicating the month for the historical period (1970-1999, first column), the future period (2040-2069, second column) and the difference (third column). The methods are shown in each row: BCCA (top row), BCSDm (middle row) and LOCA (bottom row). The fourth column show differences between future changes of each method. The rows in the fourth column represent differences between pairs of methods, LOCA-BCSDm (top row), LOCA-BCCA (middle row) and BCSDm-BCCA (bottom row).

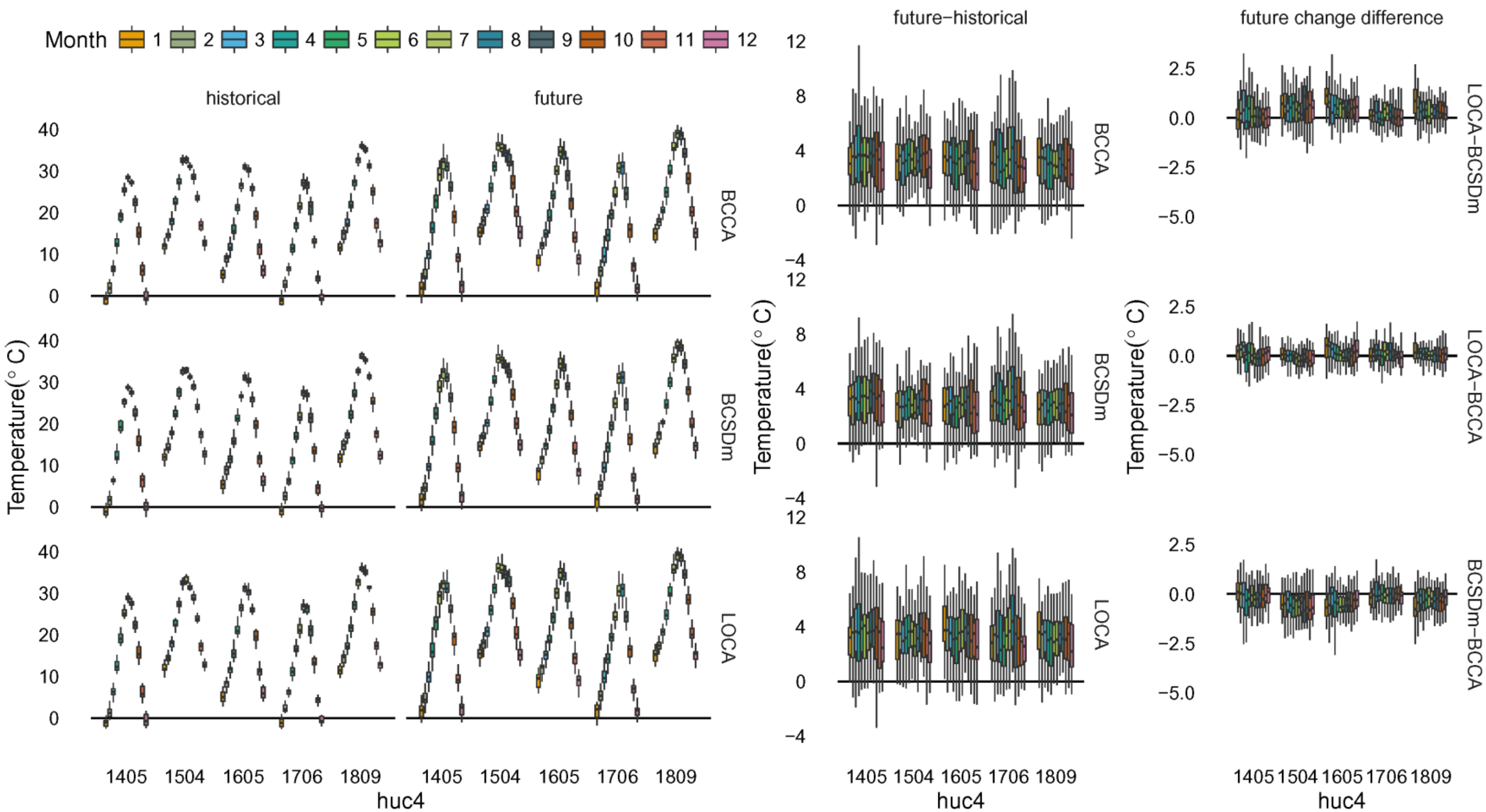

Figure 16 Boxplots of mean monthly basin average (daily value) T_{max} for 5 HUC4s, one in each of the westernmost HUC2s. Each boxplot represents the spread of all ensemble members, with the color indicating the month for the historical period (1970-1999, first column), the future period (2040-2069, second column) and the difference (third column). The methods are shown in each row: BCCA (top row), BCSDm (middle row) and LOCA (bottom row). The fourth column show differences between future changes of each method. The rows in the fourth column represent differences between pairs of methods, LOCA-BCSDm (top row), LOCA-BCCA (middle row) and BCSDm-BCCA (bottom row).

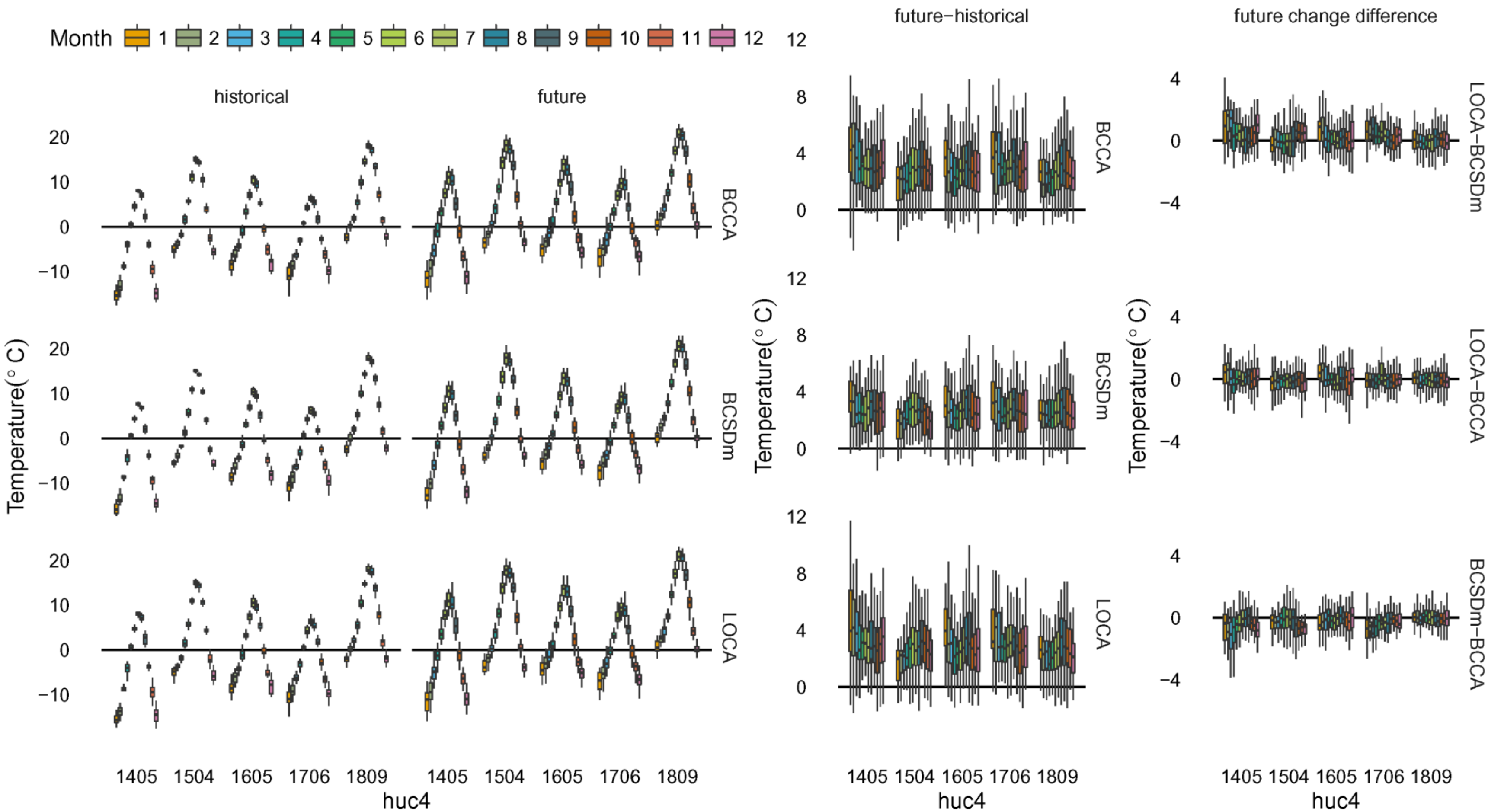

Figure 17: Boxplots of mean monthly (daily value) basin average T_{min} for 5 HUC4s, one in each of the westernmost HUC2s. Each boxplot represents the spread of all ensemble members, with the color indicating the month for the historical period (1970-1999, first column), the future period (2040-2069, second column) and the difference (third column). The methods are shown in each row: BCCA (top row), BCSDm (middle row) and LOCA (bottom row). The fourth column show differences between future changes of each method. The rows in the fourth column represent differences between pairs of methods, LOCA-BCSDm (top row), LOCA-BCCA (middle row) and BCSDm-BCCA (bottom row).

Appendix A - RCP 4.5 graphics

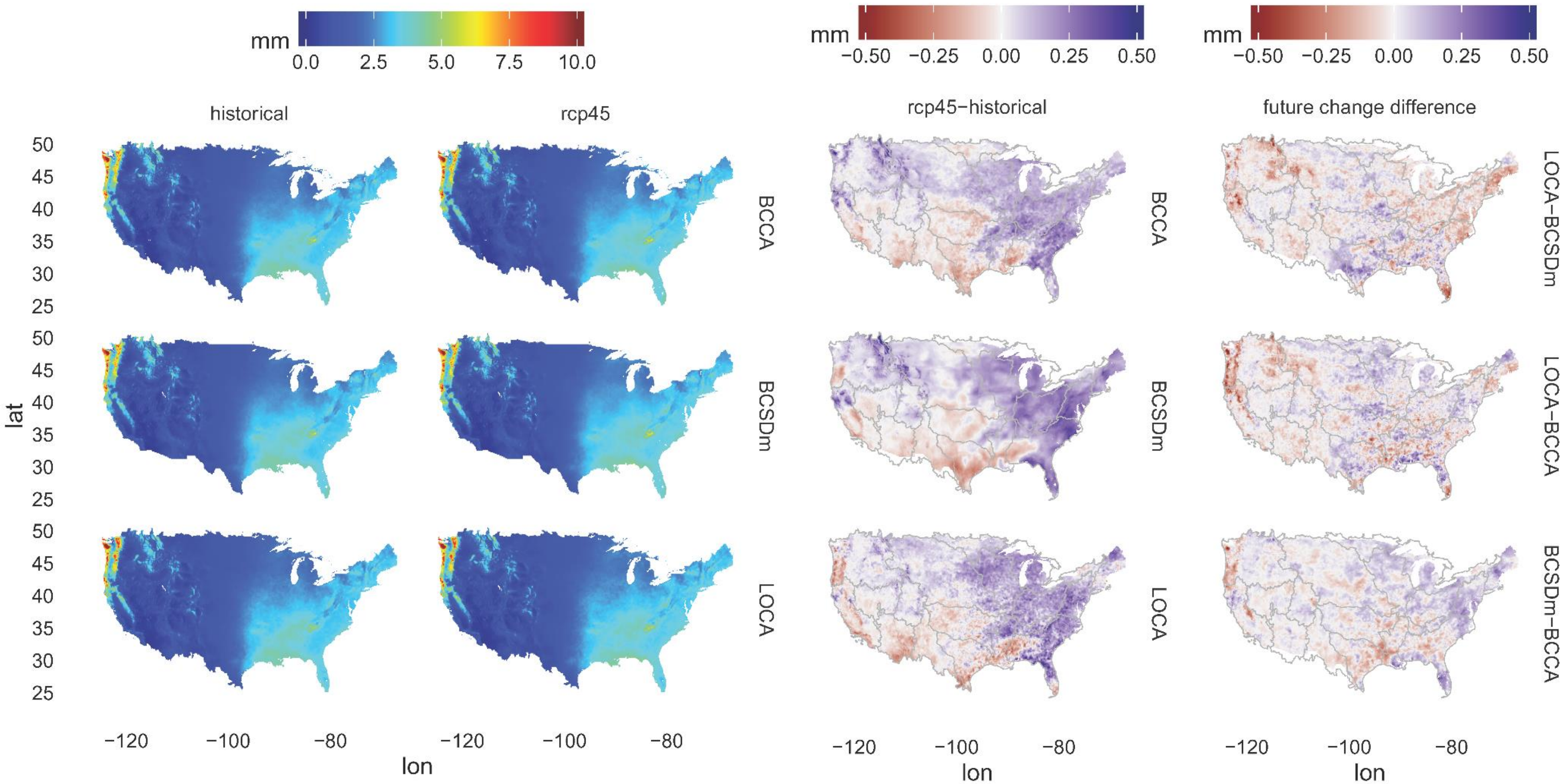

Figure A1: Ensemble median of mean daily precipitation for the historical period (1970-1999, first column), the future period (2040-2069, second column), using RCP 4.5 projections and the difference (third column). Rows correspond to each method: BCCA (top), BCSDm (middle) and LOCA (bottom). The fourth column show differences between future changes of each method. The rows in the fourth column represent differences between pairs of methods, LOCA-BCSDm (top row), LOCA-BCCA (middle row) and BCSDm-BCCA (bottom row).

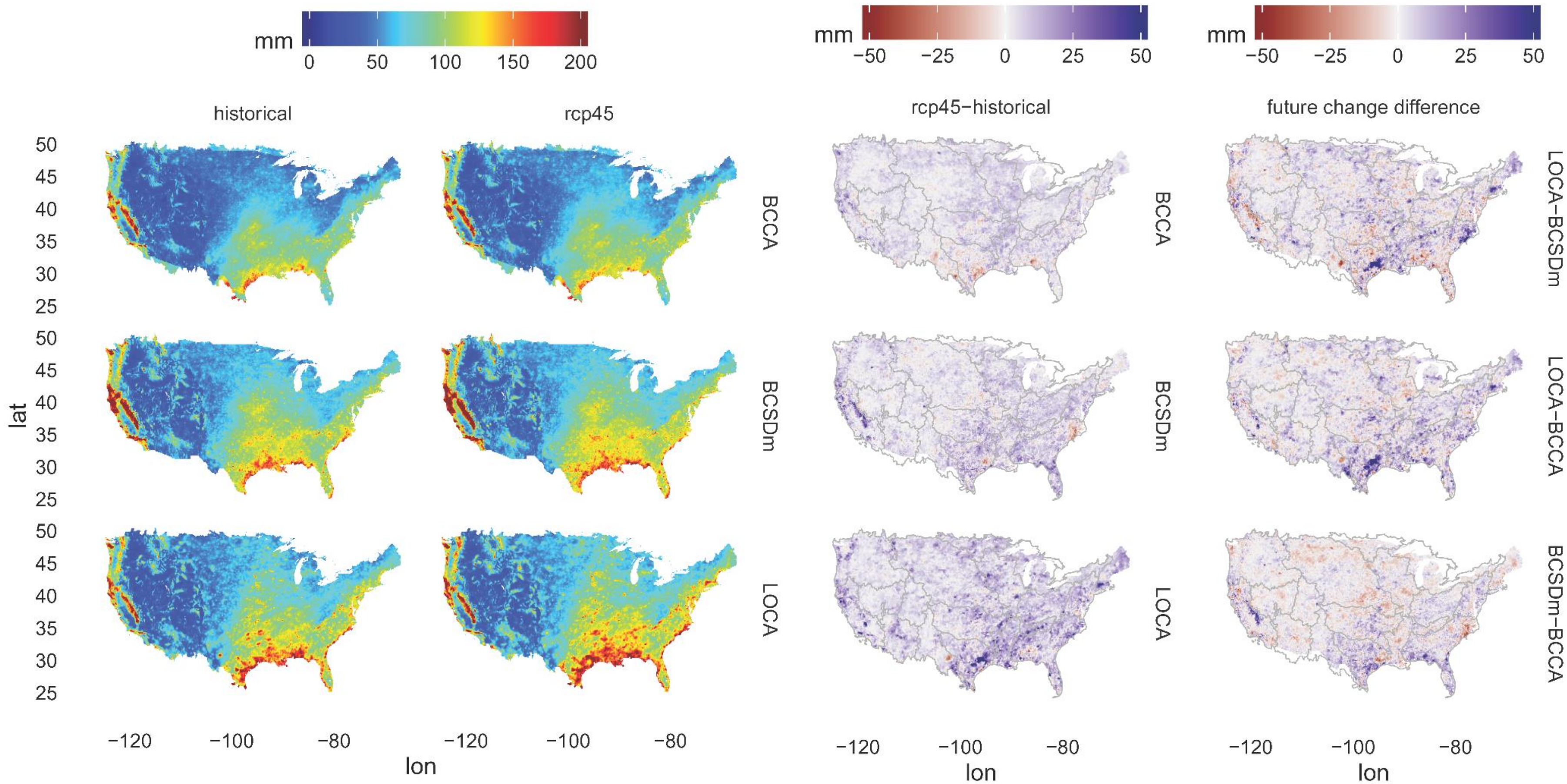

Figure A2: Ensemble median of max daily precipitation for the historical period (1970-1999, first column), the future period (2040-2069, second column) using RCP 4.5 projections and the difference (third column). Rows correspond to each method: BCCA (top), BCSDm (middle) and LOCA (bottom). The fourth column show differences between future changes of each method. The rows in the fourth column represent differences between pairs of methods, LOCA-BCSDm (top row), LOCA-BCCA (middle row) and BCSDm-BCCA (bottom row).

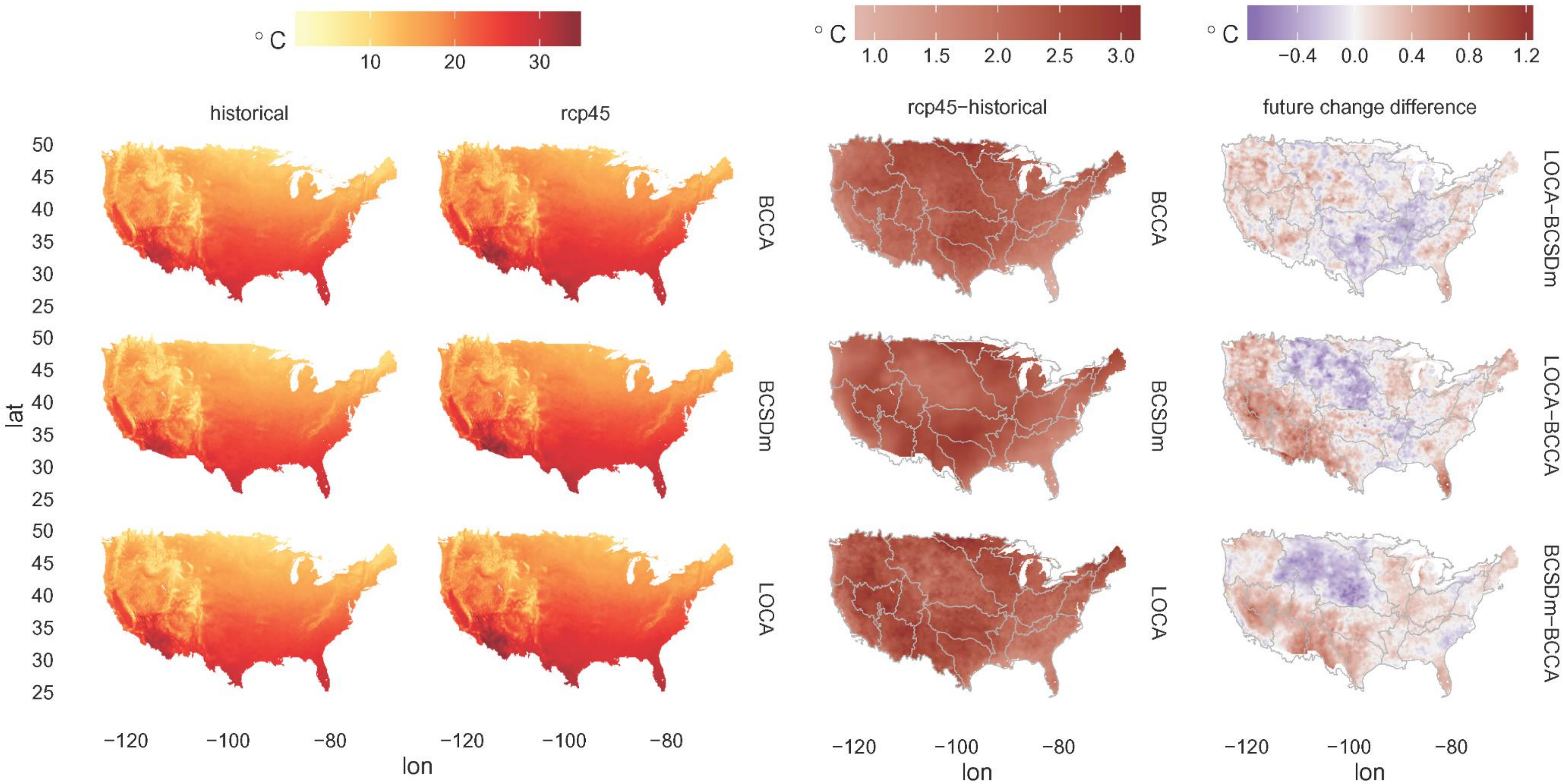

Figure A3: Ensemble median of mean daily T_{max} for the historical period (1970-1999, first column), the future period (2040-2069, second column) using RCP 4.5 projections and the difference (third column). Rows correspond to each method: BCCA (top), BCSDm (middle) and LOCA (bottom). The fourth column show differences between future changes of each method. The rows in the fourth column represent differences between pairs of methods, LOCA-BCSDm (top row), LOCA-BCCA (middle row) and BCSDm-BCCA (bottom row).

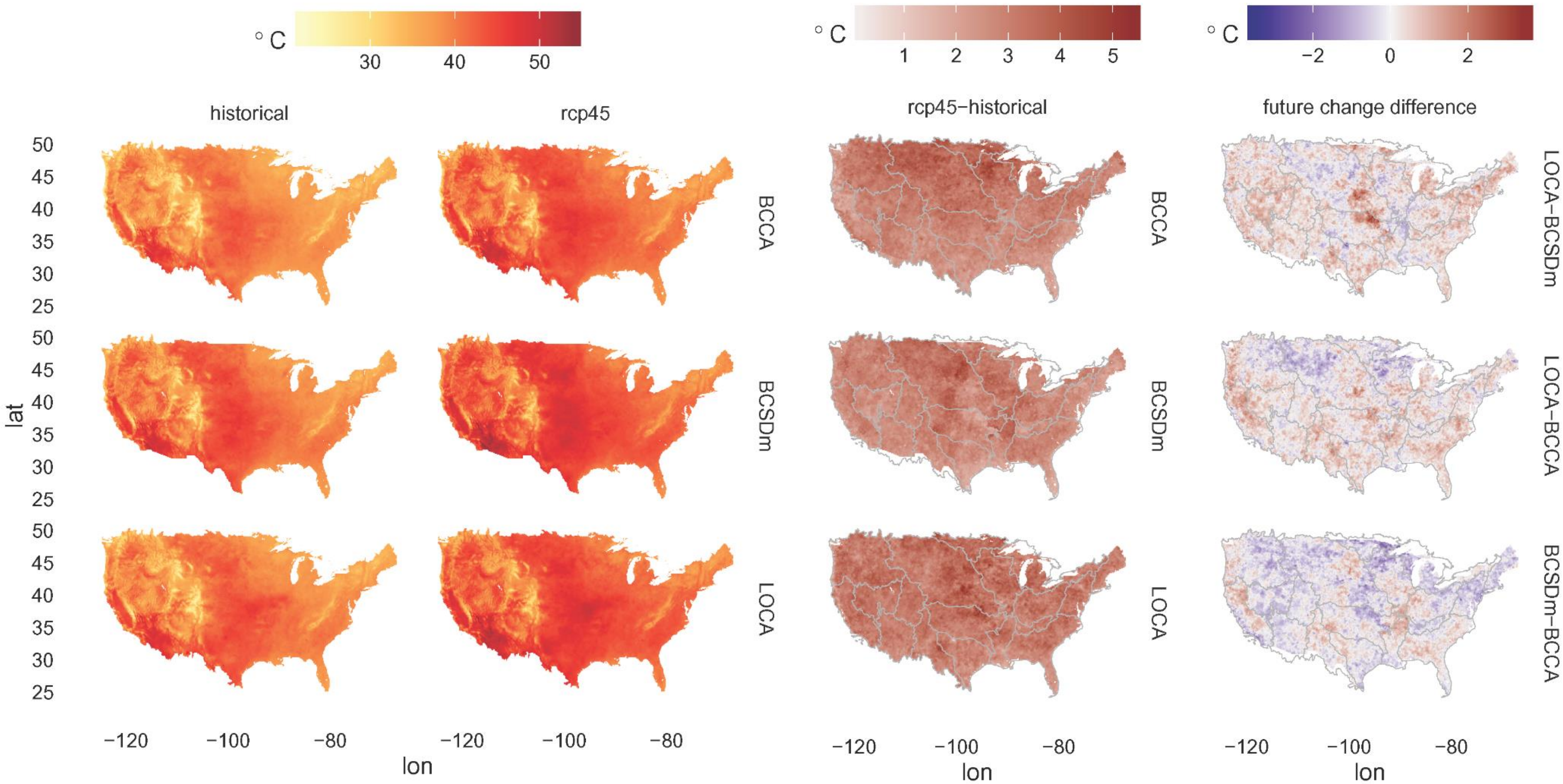

Figure A4: Ensemble median of max daily T_{max} for the historical period (1970-1999, first column), the future period (2040-2069, second column) using RCP 4.5 projections and the difference (third column). Rows correspond to each method: BCCA (top), BCSDm (middle) and LOCA (bottom). The fourth column show differences between future changes of each method. The rows in the fourth column represent differences between pairs of methods, LOCA-BCSDm (top row), LOCA-BCCA (middle row) and BCSDm-BCCA (bottom row).

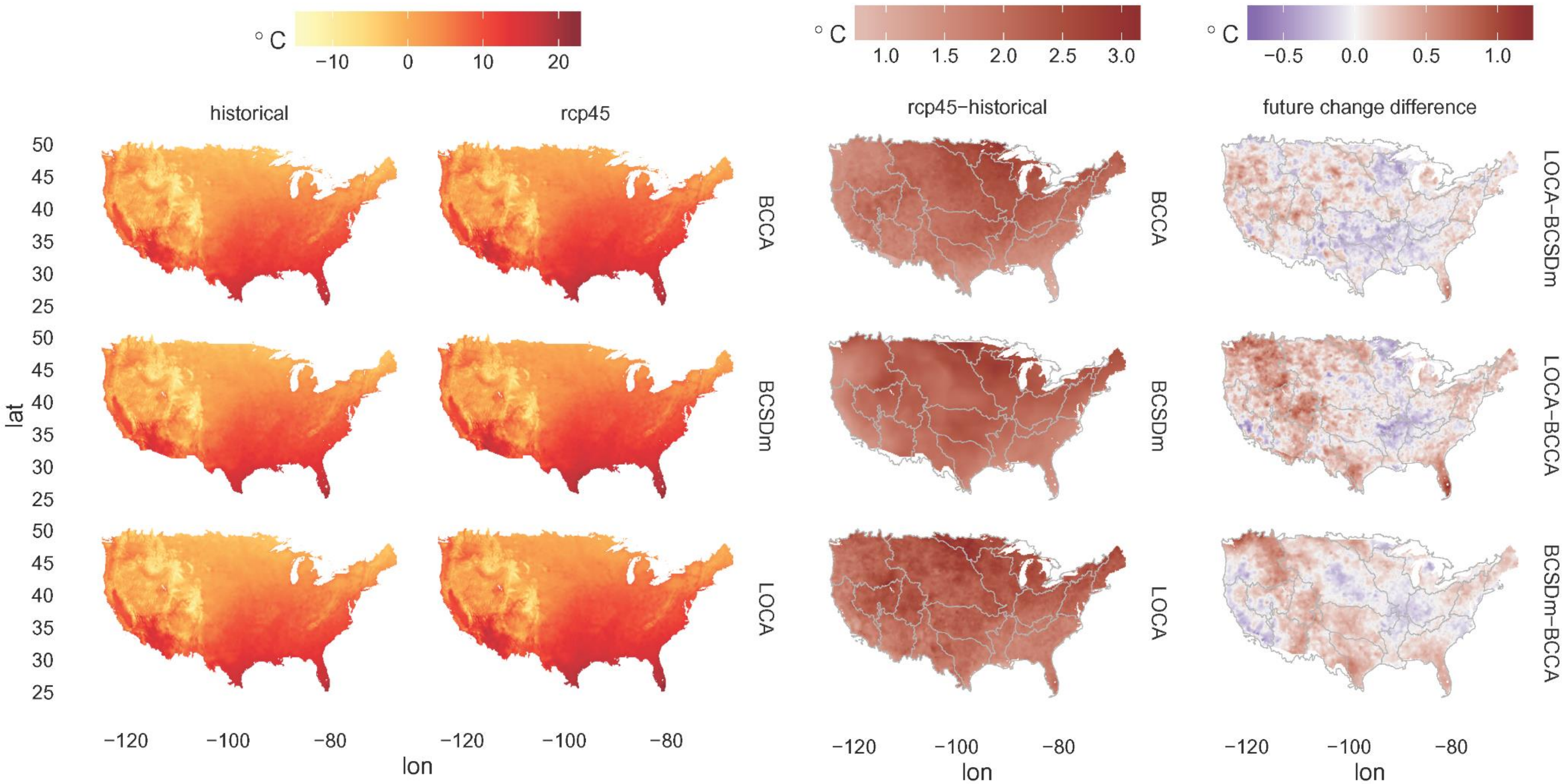

Figure A5: Ensemble median of mean daily T_{min} for the historical period (1970-1999, first column), the future period (2040-2069, second column) using RCP 4.5 projections and the difference (third column). Rows correspond to each method: BCCA (top), BCSDm (middle) and LOCA (bottom). The fourth column show differences between future changes of each method. The rows in the fourth column represent differences between pairs of methods, LOCA-BCSDm (top row), LOCA-BCCA (middle row) and BCSDm-BCCA (bottom row).

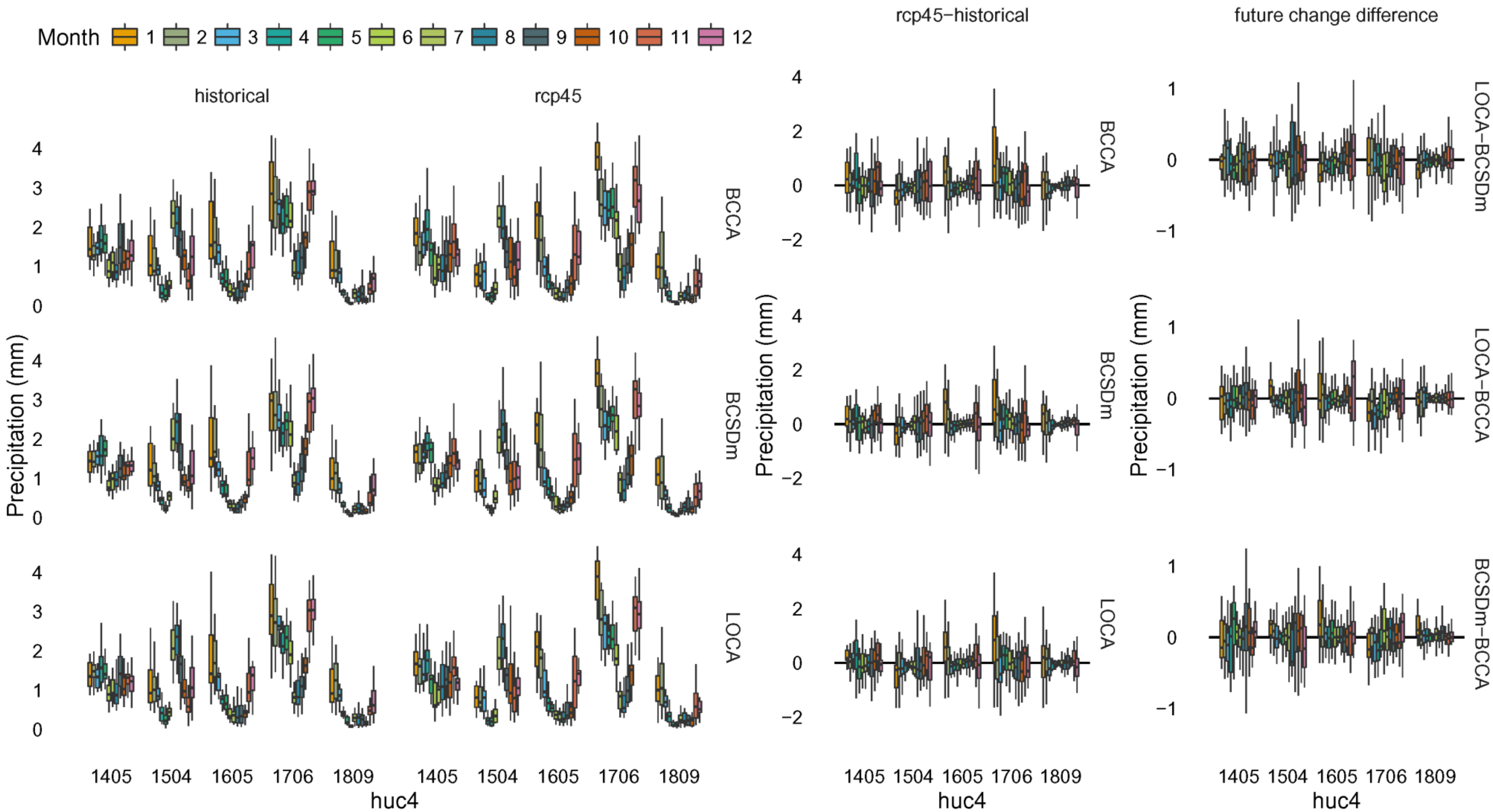

Figure A6: Boxplots of mean monthly (daily value) basin average precipitation for 5 HUC4s, one in each of the westernmost HUC2s. Each boxplot represents the spread of RCP 4.5 ensemble members, with the color indicating the month for the historical period (1970-1999, first column), the future period (2040-2069, second column) and the difference (third column). The methods are shown in each row: BCCA (top row), BCSDm (middle row) and LOCA (bottom row). The fourth column show differences between future changes of each method. The rows in the fourth column represent differences between pairs of methods, LOCA-BCSDm (top row), LOCA-BCCA (middle row) and BCSDm-BCCA (bottom row).

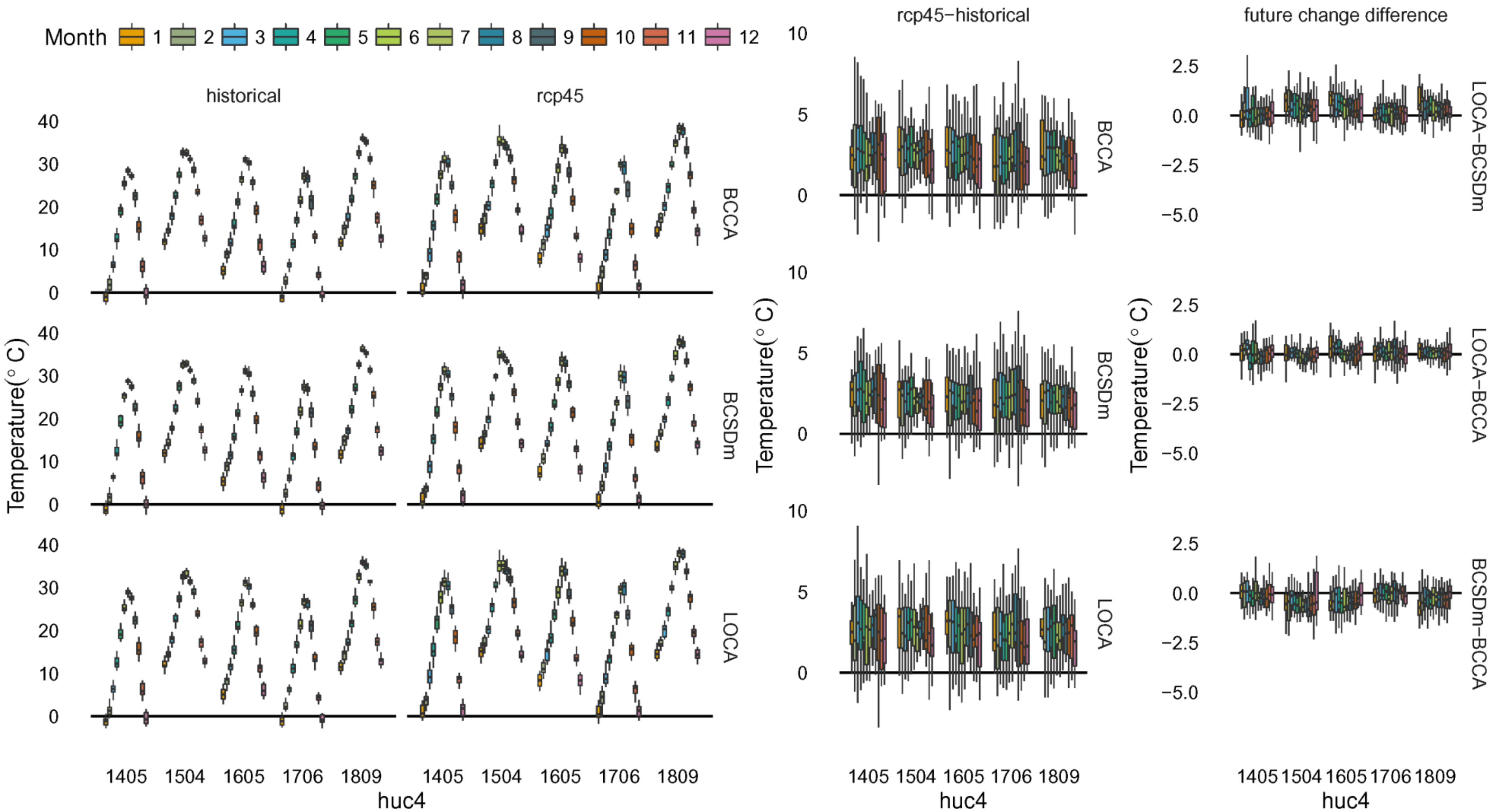

Figure A7: Boxplots of mean monthly (daily value) basin average T_{max} for 5 HUC4s, one in each of the westernmost HUC2s. Each boxplot represents the spread of RCP 4.5 ensemble members, with the color indicating the month for the historical period (1970-1999, first column), the future period (2040-2069, second column) and the difference (third column). The methods are shown in each row: BCCA (top row), BCSDm (middle row) and LOCA (bottom row). The fourth column show differences between future changes of each method. The rows in the fourth column represent differences between pairs of methods, LOCA-BCSDm (top row), LOCA-BCCA (middle row) and BCSDm-BCCA (bottom row).

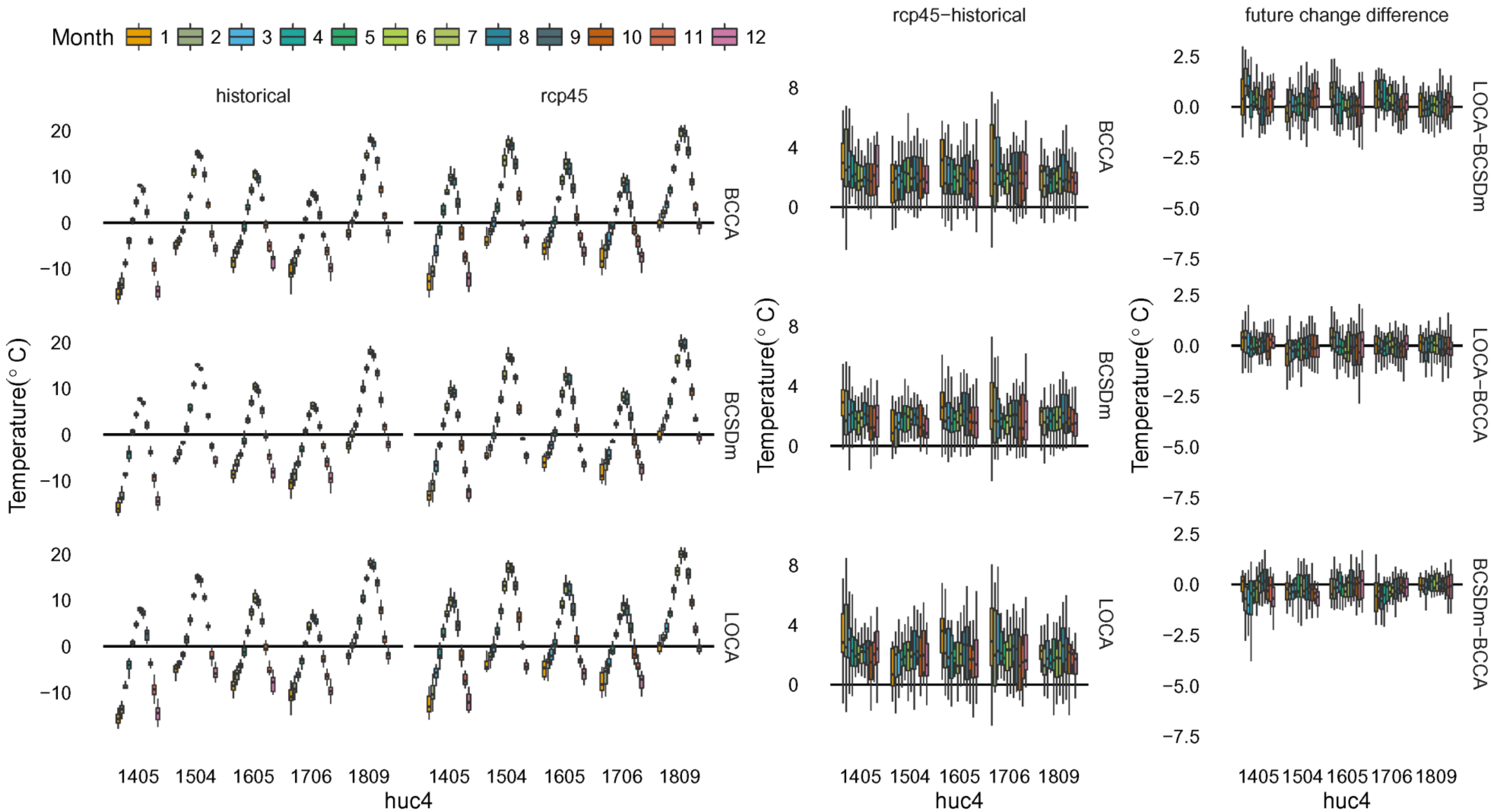

Figure A8: Boxplots of mean monthly (daily value) basin average T_{min} for 5 HUC4s, one in each of the westernmost HUC2s. Each boxplot represents the spread of RCP 4.5 ensemble members, with the color indicating the month for the historical period (1970-1999, first column), the future period (2040-2069, second column) and the difference (third column). The methods are shown in each row: BCCA (top row), BCSDm (middle row) and LOCA (bottom row). The fourth column show differences between future changes of each method. The rows in the fourth column represent differences between pairs of methods, LOCA-BCSDm (top row), LOCA-BCCA (middle row) and BCSDm-BCCA (bottom row).

Appendix B - RCP 8.5 graphics

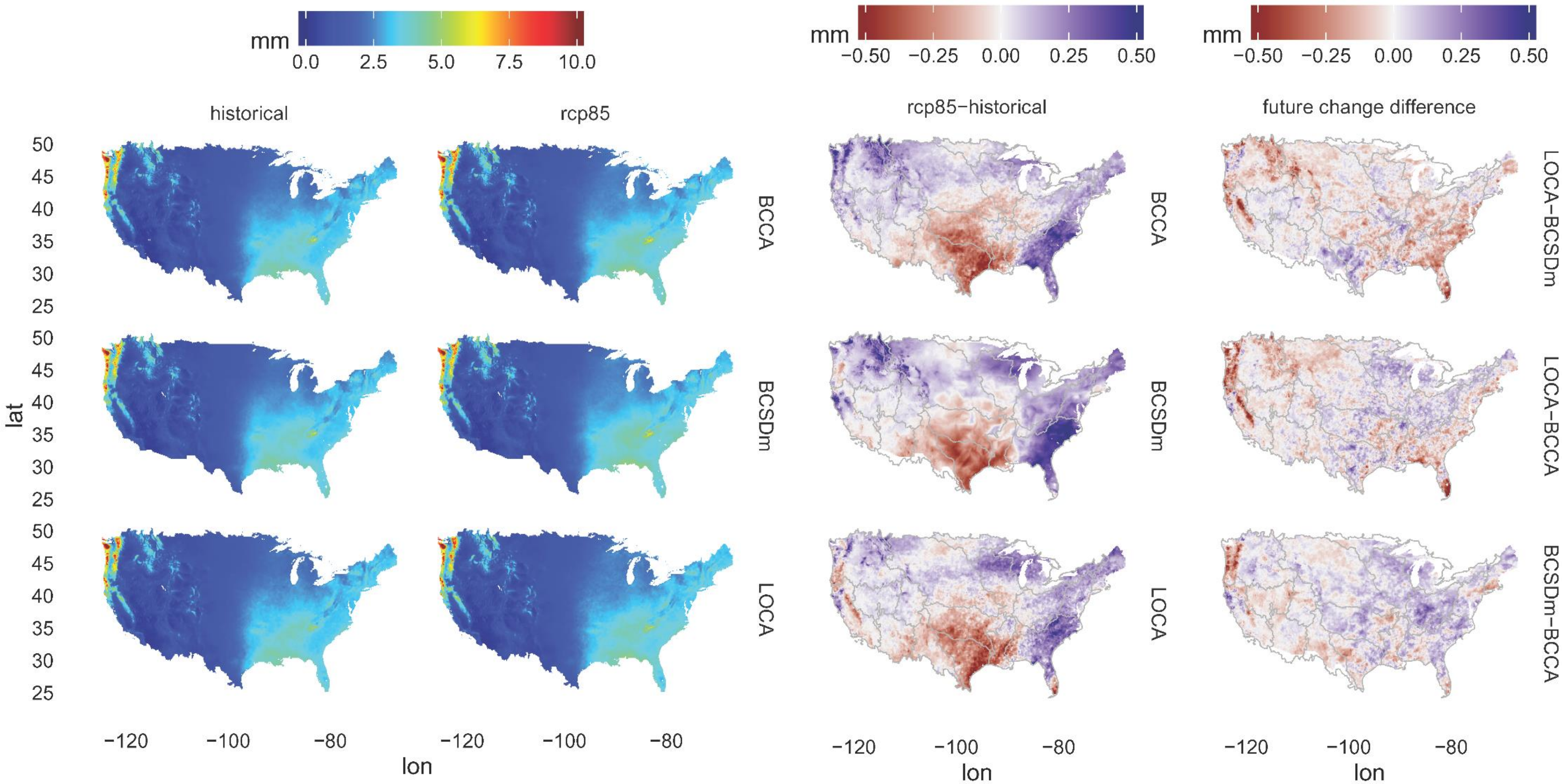

Figure B1: Ensemble median of mean daily precipitation for the historical period (1970-1999, first column), the future period (2040-2069, second column), using RCP 8.5 projections and the difference (third column). Rows correspond to each method: BCCA (top), BCSDm (middle) and LOCA (bottom). The fourth column show differences between future changes of each method. The rows in the fourth column represent differences between pairs of methods, LOCA-BCSDm (top row), LOCA-BCCA (middle row) and BCSDm-BCCA (bottom row).

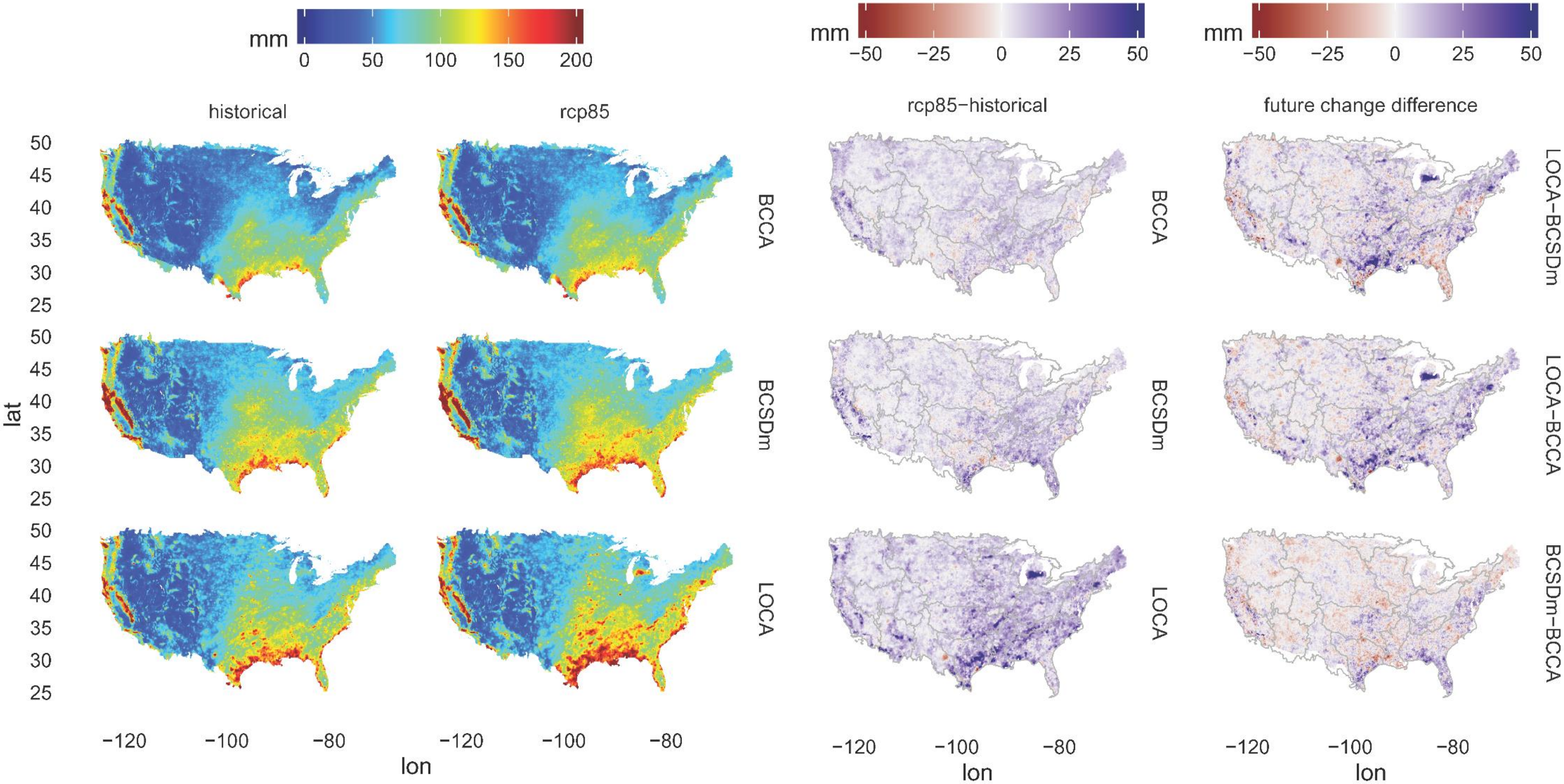

Figure B2: Ensemble median of max daily precipitation for the historical period (1970-1999, first column), the future Period (2040-2069, second column) using RCP 8.5 projections and the difference (third column). Rows correspond to each method: BCCA (top), BCSDm (middle) and LOCA (bottom). The fourth column show differences between future changes of each method. The rows in the fourth column represent differences between pairs of methods, LOCA-BCSDm (top row), LOCA-BCCA (middle row) and BCSDm-BCCA (bottom row).

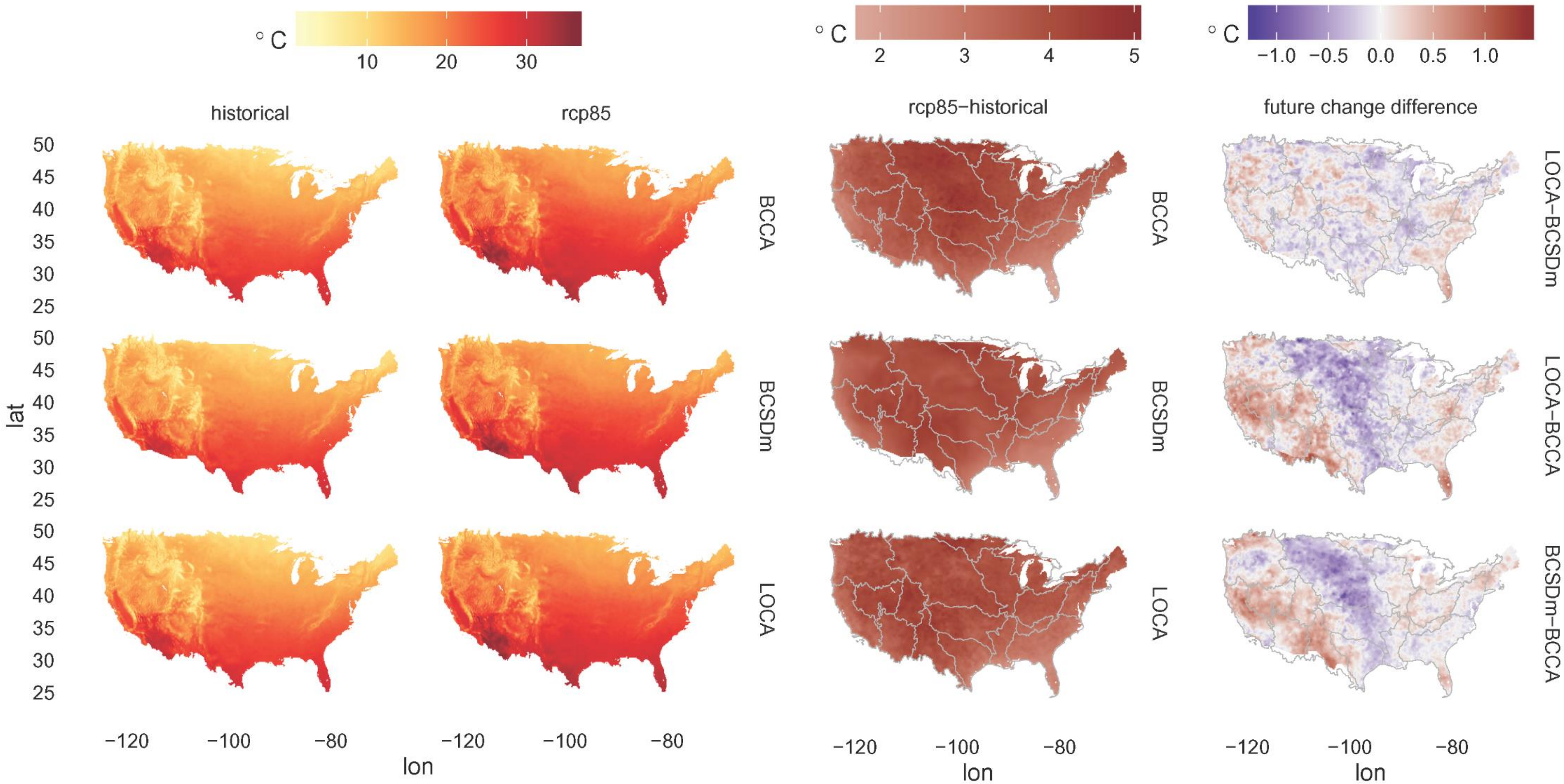

Figure B3: Ensemble median of mean daily T_{max} for the historical period (1970-1999, first column), the future period (2040-2069, second column) using RCP 8.5 projections and the difference (third column). Rows correspond to each method: BCCA (top), BCSDm (middle) and LOCA (bottom). The fourth column show differences between future changes of each method. The rows in the fourth column represent differences between pairs of methods, LOCA-BCSDm (top row), LOCA-BCCA (middle row) and BCSDm-BCCA (bottom row).

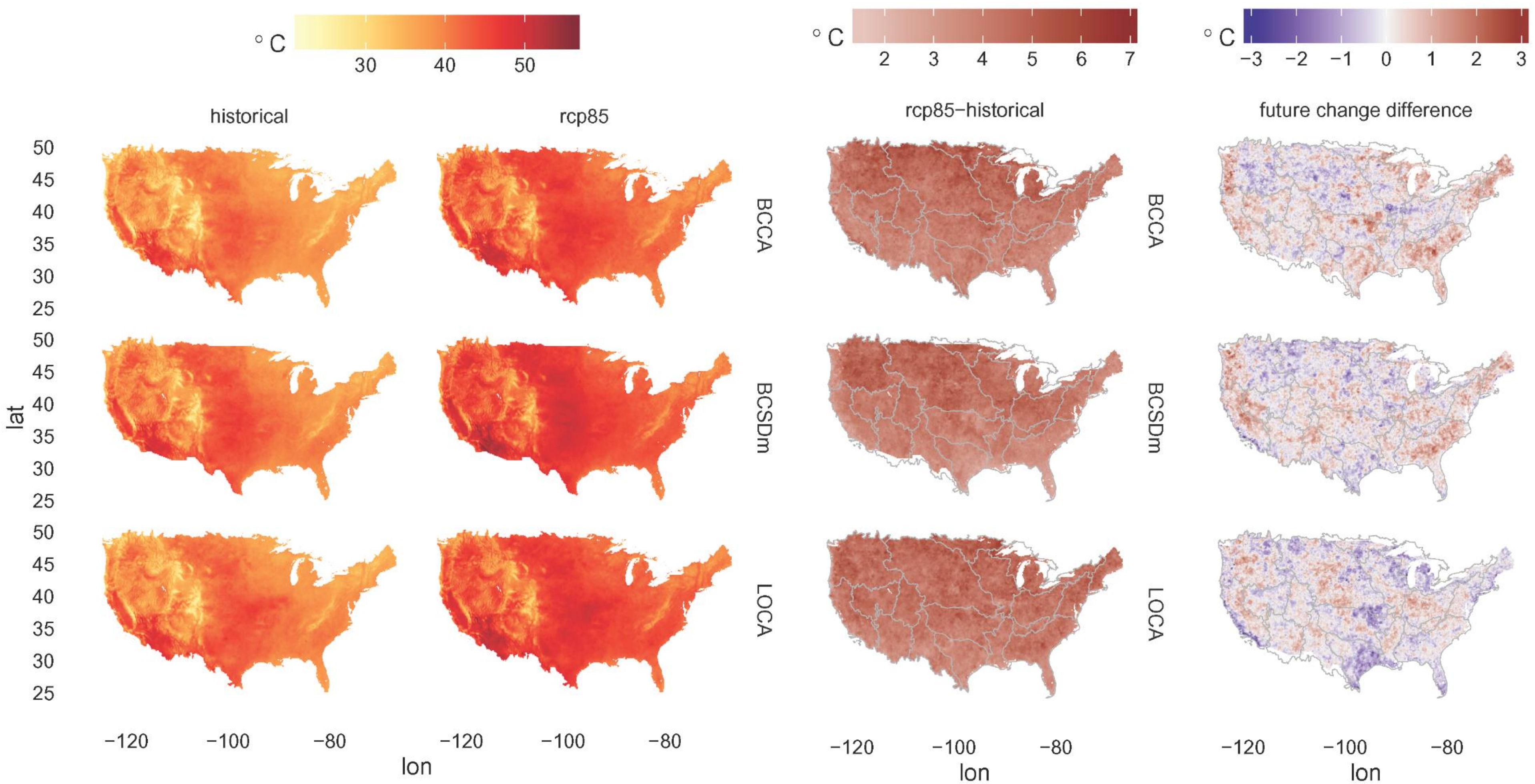

Figure B4: Ensemble median of max daily T_{max} for the historical period (1970-1999, first column), the future period (2040-2069, second column) using RCP 8.5 projections and the difference (third column). Rows correspond to each method: BCCA (top), BCSDm (middle) and LOCA (bottom). The fourth column show differences between future changes of each method. The rows in the fourth column represent differences between pairs of methods, LOCA-BCSDm (top row), LOCA-BCCA (middle row) and BCSDm-BCCA (bottom row).

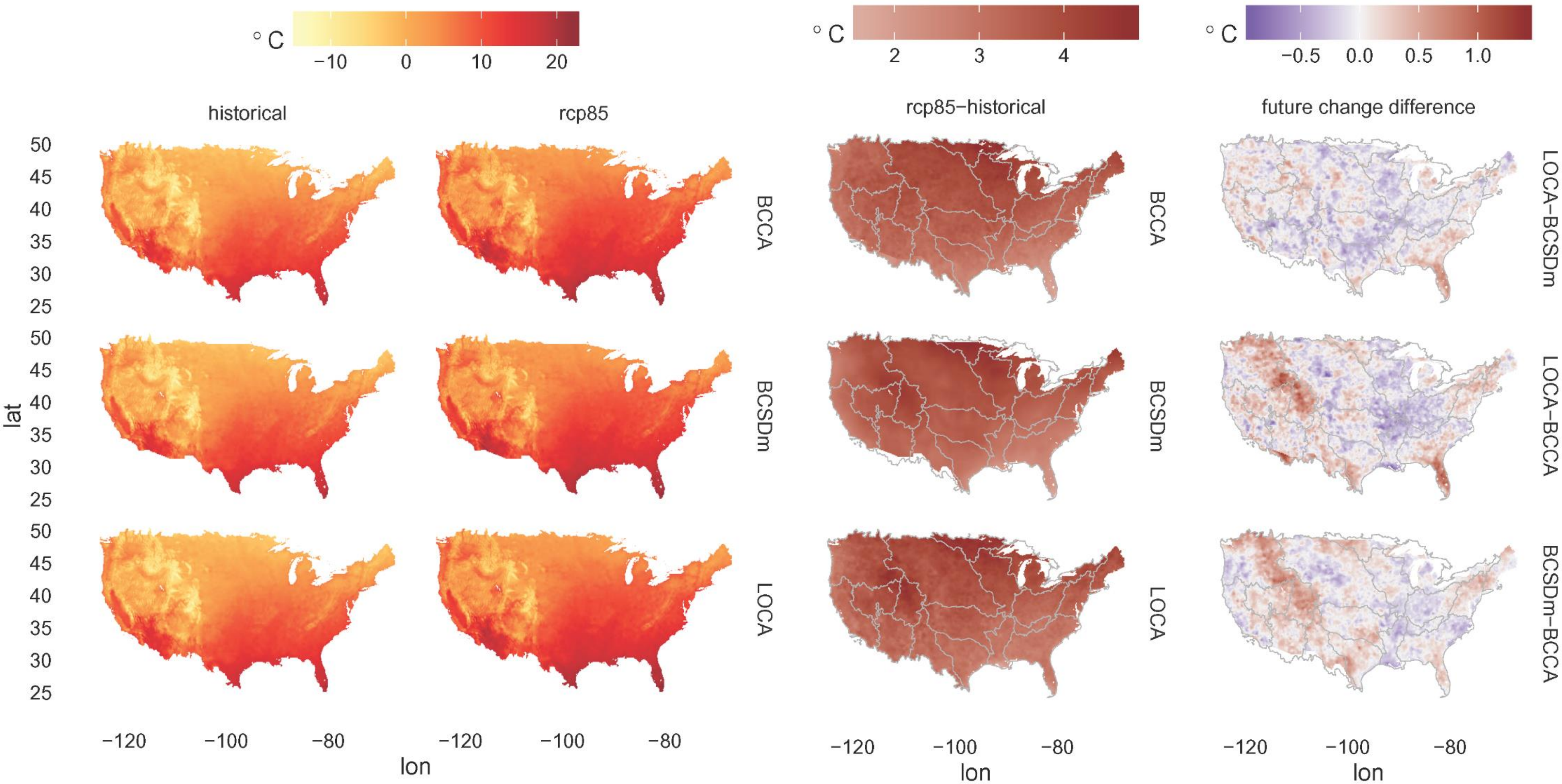

Figure B5: Ensemble median of mean daily T_{min} for the historical period (1970-1999, first column), the future period (2040-2069, second column) using RCP 8.5 projections and the difference (third column). Rows correspond to each method: BCCA (top), BCSDm (middle) and LOCA (bottom). The fourth column show differences between future changes of each method. The rows in the fourth column represent differences between pairs of methods, LOCA-BCSDm (top row), LOCA-BCCA (middle row) and BCSDm-BCCA (bottom row).

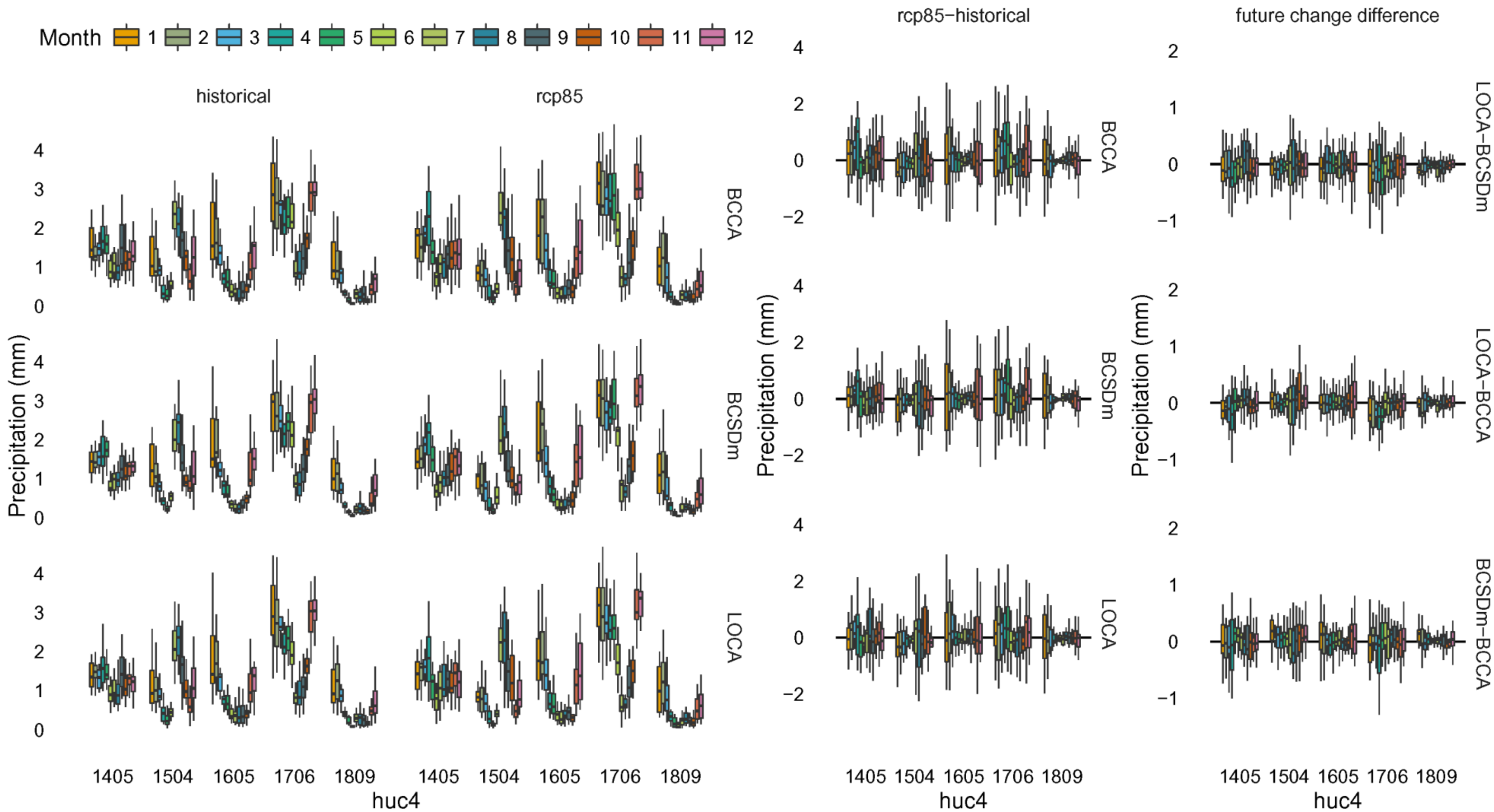

Figure B6: Boxplots of mean monthly (daily value) basin average precipitation for 5 HUC4s, one in each of the westernmost HUC2s. Each boxplot represents the spread of RCP 8.5 ensemble members, with the color indicating the month for the historical period (1970-1999, first column), the future period (2040-2069, second column) and the difference (third column). The methods are shown in each row: BCCA (top row), BCSDm (middle row) and LOCA (bottom row). The fourth column show differences between future changes of each method. The rows in the fourth column represent differences between pairs of methods, LOCA-BCSDm (top row), LOCA-BCCA (middle row) and BCSDm-BCCA (bottom row).

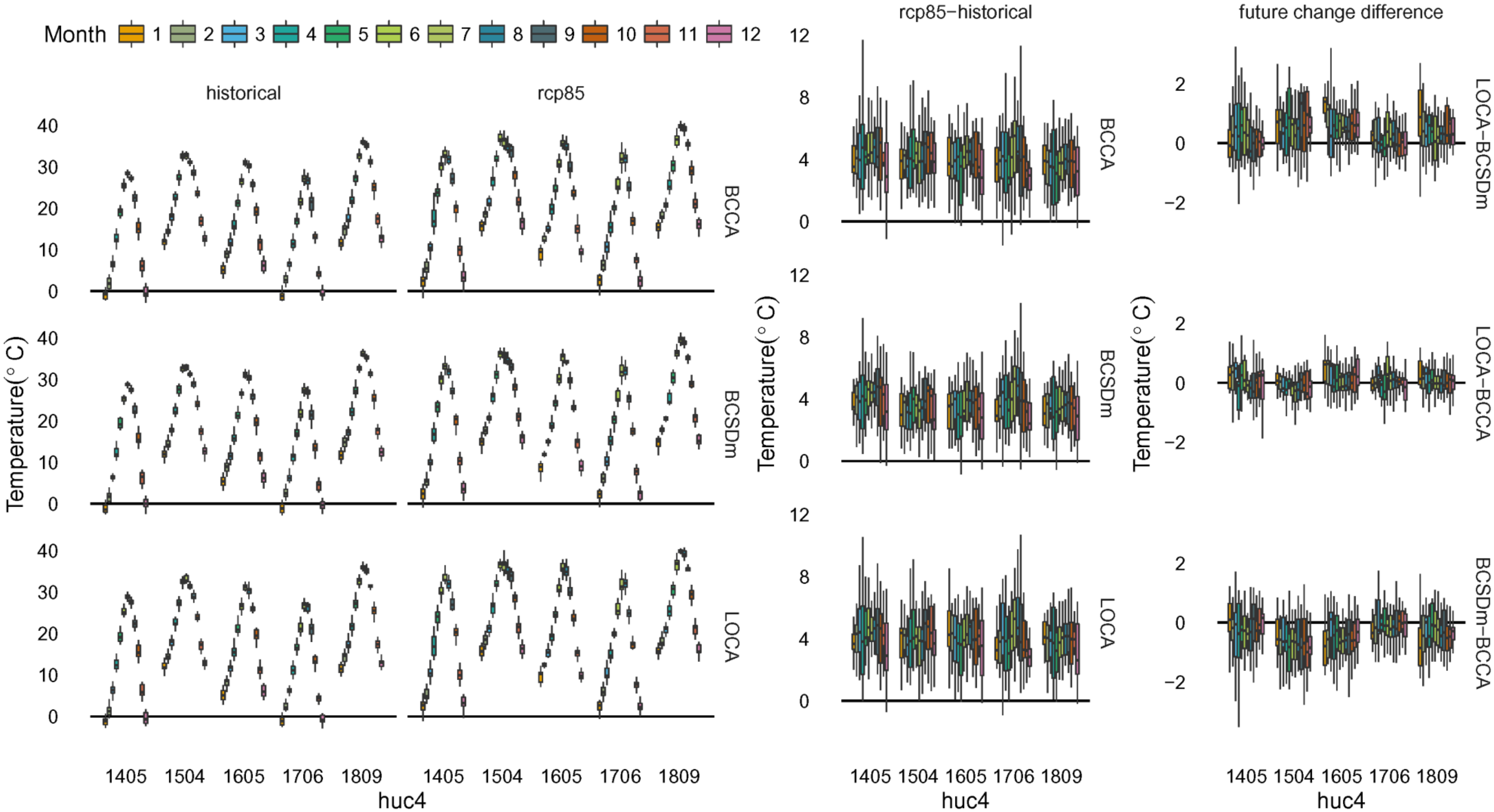

Figure B7: Boxplots of mean monthly (daily value) basin average T_{max} for 5 HUC4s, one in each of the westernmost HUC2s. Each boxplot represents the spread of RCP 8.5 ensemble members, with the color indicating the month for the historical period (1970-1999, first column), the future period (2040-2069, second column) and the difference (third column). The methods are shown in each row: BCCA (top row), BCSDm (middle row) and LOCA (bottom row). The fourth column show differences between future changes of each method. The rows in the fourth column represent differences between pairs of methods, LOCA-BCSDm (top row), LOCA-BCCA (middle row) and BCSDm-BCCA (bottom row).

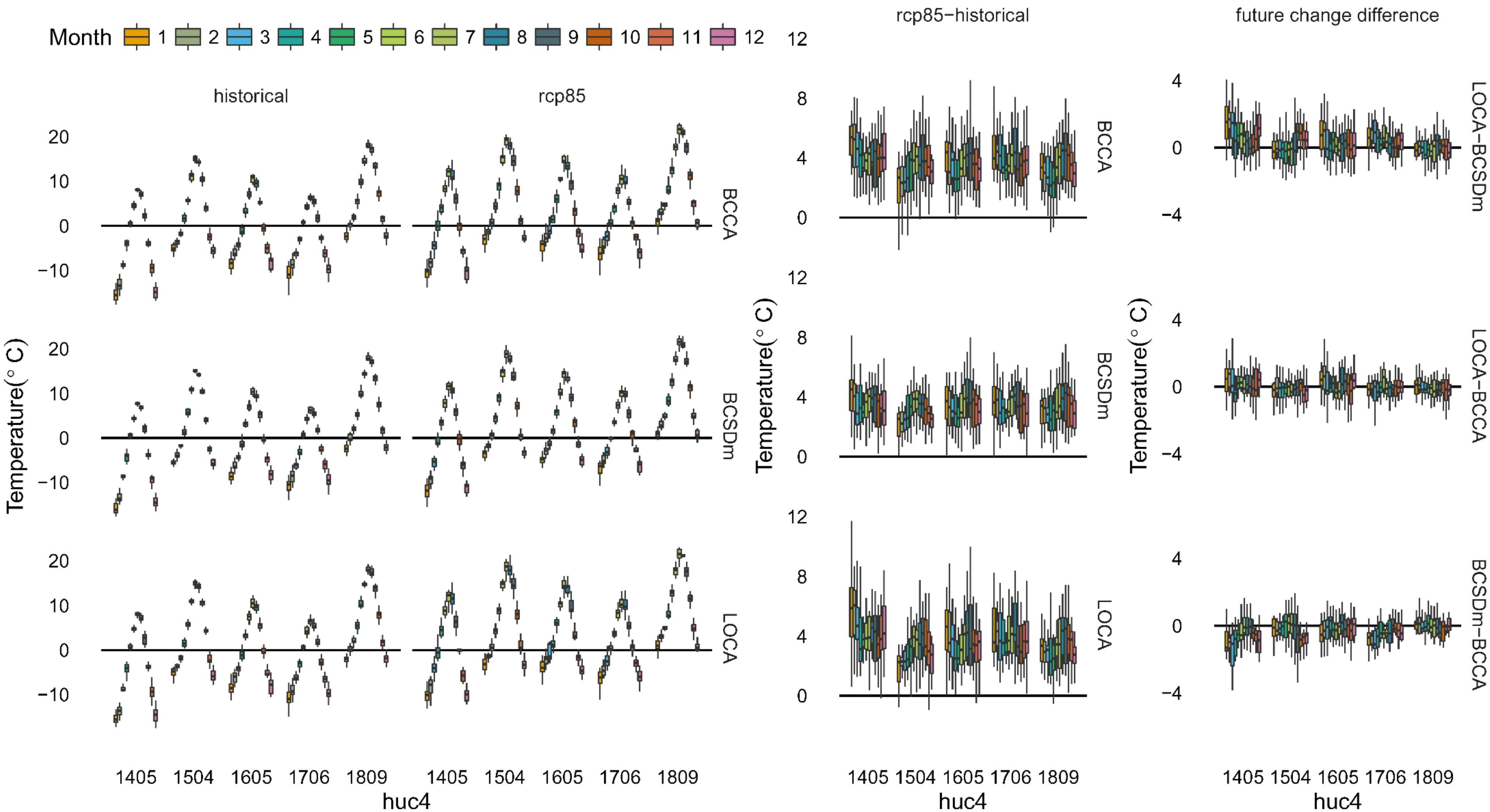

Figure B8: Boxplots of mean monthly (daily value) basin average T_{min} for 5 HUC4s, one in each of the westernmost HUC2s. Each boxplot represents the spread of RCP 8.5 ensemble members, with the color indicating the month for the historical period (1970-1999, first column), the future period (2040-2069, second column) and the difference (third column). The methods are shown in each row: BCCA (top row), BCSDm (middle row) and LOCA (bottom row). The fourth column show differences between future changes of each method. The rows in the fourth column represent differences between pairs of methods, LOCA-BCSDm (top row), LOCA-BCCA (middle row) and BCSDm-BCCA (bottom row).